Quaternary Science Reviews 270 (2021) 107145

Contents lists available at ScienceDirect

Quaternary Science Reviews

journal homepage: www.elsevier.com/locate/quascirev

Invited paper

Active North Atlantic deepwater formation during Heinrich Stadial 1

Janne Repschläger [a, *], Ning Zhao [a, b], Devin Rand [c], Lorraine Lisiecki [c], Juan Muglia [d], Stefan Mulitza [e], Andreas Schmittner [f], Olivier Cartapanis [g], Henning A. Bauch [h], Ralf Schiebel [a], Gerald H. Haug [a, i]

[a] Climate Geochemistry Department, Max Planck Institute for Chemistry, Hahn-Meitner-Weg 1, 55128, Mainz, Germany
[b] State Key Laboratory of Estuarine and Coastal Research & School of Marine Science, East China Normal University, Dongchuan Rd 500, 200241, Shanghai, China
[c] Department of Earth Science, 1006 Webb Hall, University of California, Santa Barbara, CA, 93106, USA
[d] CESIMAR, CENPAT-Conicet, 2915 Boulevard Brown, U9120ACD, Puerto Madryn, Argentina
[e] MARUM – Center for Marine Environmental Sciences, University of Bremen, Leobener Str. 8, D, 28359, Bremen, Germany
[f] College of Earth, Ocean, and Atmospheric Sciences, 104 CEOAS Admin Bldg., Corvallis, OR, 97331-5503, USA
[g] Oeschger Centre for Climate Change Research, University of Bern, Bern, Switzerland; now at CEREGE, Aix Marseille Université, CNRS, IRD, INRAE, Coll. France, Technopole Arbois, 13545, Aix en Provence, Cedex 4, France
[h] Alfred Wegener Institute, Institute for Polar and Marine Research c/o GEOMAR Helmholtz Centre for Ocean Research Kiel, Wischhofstr. 1-3, D, 24148, Kiel, Germany
[i] Department of Earth Sciences, ETH Zurich, Sonneggstrasse 5, 8092, Zurich, Switzerland

ARTICLE INFO

Article history:
Received 12 March 2021
Received in revised form
7 August 2021
Accepted 9 August 2021
Available online xxx

Handling Editor: I Hendry

Keywords:
Quaternary
Paleoceanography
North Atlantic
Data compilation stable isotopes

ABSTRACT

Deepwater circulation significantly changed during the last deglaciation from a shallow to a deep-reaching overturning cell. This change went along with a drawdown of isotopically light waters into the abyss and a deep ocean warming that changed deep ocean stratification from a salinity-to a temperature-controlled mode. Yet, the exact mechanisms causing these changes are still unknown. Furthermore, the long-standing idea of a complete shutdown of North Atlantic deepwater formation during Heinrich Stadial 1 (HS1) (17.5–14.6 kyr BP) remains prevalent. Here, we present a new compilation of benthic $\delta^{13}C$ and $\delta^{18}O$ data from the North Atlantic at high temporal resolution with consistent age models, established as part of the international PAGES working group OC3, to investigate deepwater properties in the North Atlantic. The extensive compilation, which includes 105 sediment cores, reveals different water masses during HS1. A water mass with heavy $\delta^{13}C$ and $\delta^{18}O$ signature occupies the Iceland Basin, whereas between 20 and 50°N, a distinct tongue of ^{18}O depleted, ^{13}C enriched water reaches down to 4000 m water depths. The heavy $\delta^{13}C$ signature indicates active deepwater formation in the North Atlantic during HS1. Differences in its $\delta^{18}O$ signature indicate either different sources or an alteration of the deepwater on its southward pathway. Based on these results, we discuss concepts of deepwater formation in the North Atlantic that help to explain the deglacial change from a salinity-driven to a temperature-driven circulation mode.

1. Introduction

The modern Atlantic Meridional Overturning Circulation (AMOC) in the North Atlantic is characterized by northward warm water transport near the surface, deepwater formation at high northern latitudes, and a southward return flow at depths. Modern thermohaline circulation and deep stratification are mainly driven by temperature differences between relatively warm North Atlantic Deep Water (NADW) that overlies cold Antarctic Bottom Water (AABW). Though salinity is higher in NADW, salinity differences of

* Corresponding author.
E-mail addresses: j.repschlaeger@mpic.de (J. Repschläger), nzhao@sklec.ecnu.edu.cn (N. Zhao), drand@geol.ucsb.edu (D. Rand), lisiecki@geol.ucsb.edu (L. Lisiecki), jmuglia@cenpat-conicet.gob.ar (J. Muglia), smulitza@uni-bremen.de (S. Mulitza), aschmitt@coas.oregonstate.edu (A. Schmittner), cartapanis@cerege.fr (O. Cartapanis), hbauch@geomar.de (H.A. Bauch), ralf.schiebel@mpic.de (R. Schiebel), gerald.haug@mpic.de (G.H. Haug).

https://doi.org/10.1016/j.quascirev.2021.107145

Abbreviations

ACC	Antarctic Circumpolar Current
AMOC	Atlantic Meridional Overturning Circulation
AABW	Antarctic Bottom Water
BWT	Bottom Water Temperature
CGFZ	Charlie–Gibbs-Fracture-Zone
DSOW	Denmark–Strait-Overflow-Water
DWBC	Deep Western Boundary Current
ENADW	Eastern North Atlantic Deep Water
HS1	Heinrich Stadial 1
ISOW	Iceland–Scotland Overflow Water
NADW	North Atlantic Deep Water
NAC	North Atlantic Current
LDW	Lower Deep Water
LNADW	North Atlantic Deep Water
LGM	Last Glacial Maximum
LSW	Labrador-Sea Water
MOW	Mediterranean Overflow Water
WNADW	Western North Atlantic Deep Water

0.2 between the deep NADW and AABW (Locarnini et al., 2013) play only a secondary role for deepwater stratification (Adkins, 2013; Adkins et al., 2002).

Many studies have attempted to reconstruct glacial ocean circulation using compilations of benthic $\delta^{13}C$ and $\delta^{18}O$ data (Curry and Oppo, 2005; Duplessy et al., 1980, 2002; Duplessy, 1988; Labeyrie et al., 1992, 2005; Lund et al., 2011, 2015; Lynch-Stieglitz, 2017; Lynch-Stieglitz et al., 1999, 2007, 2014; Oppo et al., 2015, 2018; Oppo and Lehman, 1993; Sarnthein et al., 1994; Tessin and Lund, 2013), neodymium isotope (ε_{Nd}) data (Colin et al., 2010; Crocker et al., 2016; Howe et al., 2018; Howe et al., 2017; Piotrowski et al., 2012; Piotrowski et al., 2008; Robinson and van de Flierdt, 2009; Zhao et al., 2019), $^{231}Pa/^{230}Th$ data (Henry et al., 2016; Lippold et al., 2016; McManus et al., 2004), ^{14}C data (Balmer and Sarnthein, 2018; Balmer et al., 2016; Ezat et al., 2019; Keigwin, 2004; Robinson et al., 2005; Skinner et al., 2010) as well as results from climate models (e.g. Ganopolski and Rahmstorf, 2001; Gebbie, 2014; Kwon et al., 2012; Muglia et al., 2018; Rahmstorf, 2002). Collectively, these studies show that glacial deepwater circulation significantly differed from the modern AMOC mode. Though the circulation rate is still discussed controversially, the main picture that evolved from these studies is a shoaling (Gebbie, 2014; Muglia and Schmittner, 2021) of the mid-depth ocean circulation (e.g. (Lynch-Stieglitz, 2017) with AABW penetrating further north and to shallower depths during the Last Glacial Maximum (LGM). Reduced connectivity between deep waters and the atmosphere may have allowed more CO_2 storage in the abyssal oceans (Sigman et al., 2010). This isolation of the abyssal ocean is thought to be driven by changes in deepwater stratification (Stein et al., 2020; Watson and Naveira Garabato, 2006) and/or inhibited air-sea exchange (Khatiwala et al., 2019). According to the deep stratification hypothesis (Adkins, 2013; Adkins et al., 2002), supported by reconstructions of deepwater salinities from pore waters, strong cooling led to homogeneous deep ocean temperatures of −2 °C during the LGM and a salinity control on deep stratification, in contrast to the modern temperature control. The reconstructed enhanced abyssal salinities were probably driven by several factors, such as a decreased freshwater input to the surface ocean by a reduction in rainfall, river run-off, and meltwater discharge (including reduced basal melting of ice shelves), as well as by more sea ice formation and associated brine rejection (Sigman et al., 2007). An asymmetric salinity increase, with a higher impact in the Southern Ocean than the North Atlantic may have reversed the modern salinity gradient between AABW and NADW, with more saline AABW occupying the deep North Atlantic basin, ocean, overlain by fresher NADW (Adkins, 2013; Adkins et al., 2002). However, pore water salinity reconstructions are sparse, their interpretation (Wunsch, 2016) and the deep stratification hypothesis (Wilmes et al., in review) have been questioned.

During the course of the deglaciation, a decrease of benthic $\delta^{18}O$ values is associated with a drawdown of the isotopically light meltwater signal from the melting ice sheets into the deep ocean through brine formation, decoupling salinity from its $\delta^{18}O$ signature (Labeyrie et al., 2005; Meland et al., 2008; Waelbroeck et al., 2011), deepwater warming (Bauch and Bauch, 2001; Cronin et al., 2000; Repschläger et al., 2015a; Skinner and Shackleton, 2006) and freshening (Adkins et al., 2002). A temperature gradient between the North Atlantic and Southern Ocean was established, while the salinity gradient between AABW and NADW reversed.

Previous research on deglacial stratification mainly focused on changes in the Southern Ocean driven by the strength and position of the Southern Ocean upwelling zone that is coupled to the extension of Antarctic sea ice and the position and strength of southern westerly winds (Menviel et al., 2018; Roberts et al., 2016; Skinner et al., 2010; Thompson et al., 2019). An increase in Southern Ocean upwelling (e.g., Knorr and Lohmann, 2003; Knorr and Lohmann, 2007), may have led to an increased CO_2 outgassing in the Southern Ocean, causing the first deglacial atmospheric warming. Furthermore, diabatic heat transport to the deep ocean and/or geothermal heating are proposed to have driven deglacial warming of the deep Southern Ocean (Ferrari et al., 2014).

In the North Atlantic, a major focus of attention has been on AMOC evolution, and most reconstructions are based on water mass distribution and mixing patterns between NADW and AABW (e.g., Oppo et al., 2015). According to climate models, AMOC strength is mainly driven by the salinity of the surface waters in the deepwater convection regions, and density gradients between the North Atlantic and Southern Ocean (Haskins et al., 2019 and citations therein). Low latitude storage of saline waters during deglacial cold events such as Heinrich Stadial 1 (HS1, 17.5 ka −14.6 ka BP), and its subsequent northward transport have been proposed to have led to strong deepwater formation and created an AMOC overshoot (Knorr and Lohmann, 2007; Liu et al., 2009). Observed decreasing $\delta^{18}O$ values are explained by a drawdown of the isotopically light meltwater by brine water formation (Waelbroeck et al., 2011) or by deepwater warming (Bauch and Bauch, 2001), inferred from benthic foraminifera and ostracod Mg/Ca records (Cronin et al., 2000; Repschläger et al., 2015a; Skinner and Shackleton, 2006). An asymmetrical warming of the deep Atlantic during HS1, compared to the other Ocean Basins is also evident in numerical models (Zhang et al., 2017).

HS1 was the major climate event at the onset of the last deglaciation associated with cold temperatures in the North Atlantic (Denton et al., 2010) and a strong meltwater outburst from various northern ice sheets (Broecker, 1994; Hemming, 2004; Naafs et al., 2013) that flushed the surface North Atlantic and capped deepwater convection sites. A long-standing concept is that deepwater convection in the North Atlantic and the associated AMOC were entirely shut down during HS1 (Duplessy, 1988; McManus et al., 2004; Rahmsdorf, 2002; Sarnthein et al., 1994) and Southern Ocean waters (Antarctic Bottom Waters) flushed the deeper whole Atlantic – a concept still prevalent in the recent literature (e.g. Böhm et al., 2015; Lynch-Stieglitz, 2017; Schmittner and Lund, 2015; Shakun et al., 2012). However, this concept has recently been challenged. Combined $\delta^{13}C$ and $\delta^{18}O$ data indicate active convection in the North Atlantic (Oppo et al., 2015) reaching down to at least

3000 m water depth in the subtropics (Repschläger et al., 2015a). While these results have questioned the idea of a complete shut-down of North Atlantic deepwater convection during HS1, the magnitude and extent of HS1-AMOC and its importance for the deglacial deepwater stratification changes remain unknown.

It is assumed that the HS1 AMOC shut-down led to the storage of warm saline waters in the upper tropical to subtropical North Atlantic. After HS1, the northward transport of warm saline tropical waters triggered the onset and overshoot of the AMOC during the Bølling-Allerød warm period (14.6–12.8 ka BP). The newly formed deepwater is supposed to have been relatively warm and saline, but this contradicts the general deglacial salinity decrease proposed by Adkins et al. (2002). The latter involving a salinity decrease of the newly formed deepwater would also prevent its sinking. To explain a deglacial freshening and warming and simultaneous increase in AMOC strength, a mechanism is needed that allows strong overturning despite the density loss by warming and freshening of the deepwater.

In order to better understand the role of the North Atlantic for water mass distribution and AMOC during the deglaciation, we have compiled published and unpublished epibenthic $\delta^{13}C$ and $\delta^{18}O$ data within the framework of the Past Global Changes (PAGES) Ocean Circulation and Carbon Cycling (OC3) working group. The improved spatial resolution of the dataset allows to trace deepwater distributions in the Atlantic Ocean and gain a better mechanistic understanding of ocean circulation changes. Here, we focus on HS1 as the major climate event in during the early deglaciation with the following research questions: (1) Was there active deepwater formation in the North Atlantic during HS1? (2) What role did HS1 in the North Atlantic play for the reconstructed changes in deepwater salinity and stratification?

2. Modern oceanography

Deepwater formation in the subpolar North Atlantic occurs in two main convection areas, the Nordic Seas, the Labrador Sea (Lherminier et al., 2010; Sarafanov et al., 2012; Schmitz and McCartney, 1993; Xu et al., 2010), supplemented by convection and subduction in the Irminger and Iceland basins (Pickart et al., 2003; Sarafanov et al., 2012). Additional deepwater formation occurs in the Mediterranean Sea, which contributes to the Atlantic mid depth circulation (Lozier and Stewart, 2008; van Aken, 2000a, 2001).

Deepwaters formed in the Nordic Seas leave the area via shallow sills, the Faroe Bank Channel (Chafik et al., 2020) and Denmark Strait as Iceland Scotland Overflow Water (ISOW) and Denmark Strait Overflow Water (DSOW), respectively (Hansen et al., 2016; Hansen and Østerhus, 2000; Lherminier et al., 2010; Macrander et al., 2005; Sarafanov et al., 2012; Schmitz and McCartney, 1993; Schott et al., 2004; Schott and Brandt, 2013; Våge et al., 2011; Xu et al., 2010). With a flux of about 3 Sv, ISOW flows southward across the Iceland-Scotland Ridge (Sarafanov et al., 2012; Chafik et al., 2020) into the Iceland Basin, propagates along the eastern flank of Reykjanes Ridge and mixes with and entrains deepwater formed in the Iceland Basin (0.6 Sv) (Sarafanov et al., 2012). At Charlie-Gibbs fracture zone (CGFZ), a minor portion of ISOW continues southward along the Mid Atlantic Ridge (MAR) and form Eastern North Atlantic Deep Water (ENADW), which occupies water depths of 1500–3000 m (Sarafanov et al., 2012; van Aken, 2000a; Van Aken and De Boer, 1995).

The main branch of ISOW (3.8 Sv) flows through CGFZ into the Irminger Basin (Sarafanov et al., 2012), where a smaller branch turns southward while the major volume flows northward along Reykjanes Ridge (Våge et al., 2011) into the Irminger Basin. This northward deepwater flow is deflected by the Greenland-Iceland Ridge, and partially mixes with the DSOW that spills into the Irminger Basin via the Denmark Strait. The combined water mass called Western North Atlantic Deep Water (WNADW) is underlain by the colder, denser pure DSOW. Both DSOW and WNADW get further mixed on their southward way along the contours of the Greenland slope, and anticlockwise circulation in the Labrador Basin. The combined outflow of DSOW and WNADW from the Labrador Sea combines partially with Labrador Sea Water and into the Deep Western Boundary Current (DWBC) (Fischer et al., 2004, 2015). The DWBC flows around the Flemish Cap back into the western North Atlantic basin and further along the continental slope of eastern North America. The combined northern source water described above, typically called Lower North Atlantic Deep Water (LNADW), fills the deep North Atlantic below about 2000 m to abyssal depths. To the south of about 40°N, and more prominently in the South Atlantic, LNADW is underlain by northward moving AABW (Curry et al., 2003). The boundary between LNADW and AABW progressively shoals towards the south. At about 50°S, NADW starts to resurface, is partially entrained into the Antarctic Circumpolar Current (ACC), and contributes to AABW formation (Marshall and Speer, 2012; Talley, 2013).

The cold dense NWADW is overlain by LSW forming in the Labrador Sea and the southwestern Irminger Sea (Pickart et al., 2003) from a mixture of saline Irminger Current and fresh cold East Greenland Current waters. LSW formation is favored by the cold dry winds originating from the partially ice-covered continental landmasses surrounding the Labrador Sea leading to winter convection. LSW is less dense than ISOW, typically occupies water depths between 500 m and 1500 m, but can even reach down to 2200 m during years with strong deepwater convection (Faure and Speer, 2005; Yashayaev, 2007; Yashayaev and Loder, 2009). LSW contributes 7.8 Sv to the total AMOC deep-water export of 13 Sv (Sarafanov et al., 2012).

Deepwater circulation in the eastern North Atlantic basin south of the CGFZ differs from its western counterpart by a lower contribution of ENADW. Mediterranean Outflow Water (Curry et al., 2003) occupies the mid water depth instead of LSW, and direct flushing with AABW into the eastern Atlantic Basin is prevented by the Walvis Ridge. Instead, AABW enters the East Atlantic Basin via Vema fracture zone at 11° N (Van Aken, 2000; Van Aken and De Boer, 1995). Entrainment of the overlying water masses modifies AABW slightly, thus is called Lower Deepwater (LDW) in the East Atlantic Basin. LDW and ENADW are overlain by Mediterranean Overflow Water. The latter is formed in Mediterranean Sea by high evaporation rates that lead to a salinity increase and the formation of a relatively warm (11 °C) and saline (36) (Locarnini et al., 2013) deep water mass (Marshall and Schott, 1999). MOW enters the Atlantic via the Strait of Gibraltar and typically occupies depth between 700 and 1700 m in the Eastern to Central North Atlantic between 30°N and 50°N (Baringer and Price, 1997; Lozier and Stewart, 2008).

3. Methods

This compilation of published and unpublished benthic foraminifera $\delta^{13}C$ and $\delta^{18}O$ data focusses on the Atlantic section north of the equator, yet records from the South Atlantic are also included. The compilation is a product of the PAGES OC3 working group (Schmittner et al., 2017), which aims to better understand past changes in ocean circulation and carbon storage. The presented North Atlantic dataset includes 105 cores. The compilation is updated from a personal raw data compilation by O. Cartapanis, supplemented with data from the PALMOD compilation (Jonkers et al., 2020), and additional published and unpublished (cores MSM58-52-02 and core KNR197-10_GGC5) deglacial sites. All data

were quality-controlled revisiting the original publications (Abrantes et al., 1998, 2018; Bauch et al., 2001; Bertram et al., 1995; Beveridge et al., 1995; Bickert and Mackensen, 2004; Boyle and Keigwin, 1985; Cacho et al., 2006; Came et al., 2008; Chi and Mienert, 2003; Collins et al., 2010; Curry et al., 1988, 1999; Curry and Oppo, 1997; Dickson et al., 2009; Duplessy, 1982, 1988; Elliot, 2017; Elmore and Wright, 2011; Elmore et al., 2015; Fink et al., 2013; Freudenthal et al., 2002; Frigola et al., 2008; Gersonde et al., 2003; Hagen et al., 2002; Hagen and Keigwin, 2017; Hillaire-Marcel et al., 1994; Hoffman and Lund, 2012; Hoogakker et al., 2015; Hüls, 1999; Jansen and Veum, 1990; Jonkers et al., 2015; Jung, 1996; Keigwin and Jones, 1994; Keigwin, 2004; Keigwin et al., 1991; Keigwin and Lehman, 1994; Keigwin and Schlegel, 2002; Keigwin and Swift, 2017; Kiefer, 1998; Labeyrie et al., 1995, 1999; Labeyrie, 1996; Lebreiro et al., 2009; Little et al., 1997; Lund et al., 2015; Lynch-Stieglitz et al., 2011; Mackensen, 2001; Manighetti et al., 1995; Members, 1976, 2004, 2004; Middleton et al., 2016, 2018; Millo, 2005; Millo et al., 2008; Mulitza et al., 2008, 2017; Nam, 1997; Oppo et al., 2006, 2015; Oppo and Fairbanks, 1990; Oppo and Horowitz, 2000; Oppo and Lehman, 1995; Pichevin et al., 2005; Praetorius et al., 2008; Repschläger et al., 2015a; Richter, 1998; Rickaby and Elderfield, 2005; Sarnthein et al., 1988, 1994; Schwab et al., 2012; Shimmield, 2004; Sierro et al., 2005; Slowey and Curry, 1995; Telesiński et al., 2014; Thornalley et al., 2010, 2011; Tiedemann, 1991; Tjallingii et al., 2008; van Kreveld et al., 2000; Vidal et al., 1997; Voelker et al., 2006; Vogelsang et al., 2001; Voigt et al., 2017; Waelbroeck et al., 2001, 2006, 2011, 2019; Weinelt, 1993; Weldeab et al., 2016; Willamowski, 1999; Zabel et al., 2001; Zahn et al., 1987; Zarriess et al., 2011; Zarriess and Mackensen, 2011; Zhang et al., 2015). The detailed list for the quality check is given in the supplementary information and included revisiting the original data, controlling first authorship of data, species names standardization, control of potential species offset corrections and age model revisions.

For $\delta^{18}O$ measurements, offsets have been reported (Hodell et al., 2003; Ostermann and Curry, 2000; Waelbroeck et al., 2005) and are discussed in detail in Waelbroeck et al. (2005). Several factors my influence the measurements and lead to inter-laboratory offsets. These are differences in 1) sample treatment prior to analyses, 2) in measurement methods, and 3) in calibration against the standards. The influence of different cleaning methods, plasma ashing (roasting), chemical treatment with ethanol/methanol, oxygen peroxide (H_2O_2), sodium hypochlorite (NaOCl), Sodiumpyrophosphate or Calgon have been investigated (Feldmeijer et al., 2013; Mead et al., 1993; Serrano et al., 2008) and showed a systematic lowering of the $\delta^{18}O$ value when cleaned with H_2O_2 (Serrano et al., 2008), with a maximal derivation of 0.18‰ in the $\delta^{18}O$ signal.

Main differences between $\delta^{18}O$ measurements have been reported between laboratories using a common acid bath (Shackleton and Opdyke, 1973) e.g. referred to as VG-ISOCARB and laboratories using a single acid aliquot method that is mainly referred to as automatic carbonate preparation device and coupled to a mass spectrometer. The single acid aliquot method is more recently also used in modern gas bench systems (e.g., Vonhof et al., 2020). For the common acid bath −0.4‰ lighter $\delta^{18}O$ values in comparison to the single acid aliquot method have been reported. This difference is probably related to the reaction time of the samples in the acid bath and the timing of CO_2 extraction (Hodell et al., 2003) and was solved by decreasing the extraction time (see summary in Waelbroeck et al., 2005). No additional publications on this matter have been issued, thus we assume that these inter-laboratory calibration problems have been solved internally and not been reported in any publications.

Problems with calibrations of internal vs in house standards versus quality control standards have been reported and solved (Ostermann and Curry, 2000). Sample size depending fractionation (Vonhof et al., 2020, and citations therein) as well as the lack of a standard that allows sample calibration for values higher than 4‰ may add additional uncertainty to the measurements.

To exclude an overinterpretation of the compiled datasets an error of 0.2‰ should generally be considered as also proposed by Waelbroeck et al. (2005). To test the dataset for laboratory offsets, we checked the $\delta^{18}O$ records from the late Holocene times slice (Figure S1). Though the standard deviation of LH samples partially exceeded the 0.2‰ range, no systematic offset to lighter values from laboratories using a common acid bath could be detected.

The $\delta^{18}O$ of *C. wuellerstorfi* and *U. peregrina* is characterized by an offset (Duplessy et al., 1984; Shackleton and Opdyke, 1973). It has been assumed that the epifaunal *C. wuellerstorfi* secretes its calcite in disequilibrium with ambient seawater due to vital effects. Therefore, the $\delta^{18}O$ of *C. wuellerstorfi* is corrected for vital effects by 0.64‰ to match *U. peregrina*. More recently, this procedure has been revised as the infaunal *U. peregrina* has been found to also secrete its calcite in disequilibrium with ambient pore water (Marchitto et al., 2014). Vital effects and species offsets for $\delta^{13}C$ are even stronger and less systematic in epifaunal and infaunal species (Fontanier et al., 2006). In order to avoid any systematic errors by corrections for vital effects, all data presented here are based on epifaunal *Cibicidoides* specimen $\delta^{18}O$ and $\delta^{13}C$ data without vital effect corrections. All $\delta^{18}O$ and $\delta^{13}C$ data are based on observations from foraminiferal calcite ($\delta^{18}O_{cc}$ and $\delta^{13}C_{cc}$) and are displayed against the V-PDB scale for all stable isotope data hence forward. This signal still includes the effect of water temperature and global ice volume changes. To transfer $\delta^{18}O_{cc}$ into $\delta^{18}O$ of seawater ($\delta^{18}O_{sw}$), water temperature reconstructions would be needed. The latter are not available for most records, thus, $\delta^{18}O_{cc}$ distributions are presented in the results and the effect of temperature and ice volume changes is presented in the discussion.

$\delta^{13}C_{cc}$ of *Cibicidoides* represent the $\delta^{13}C$ of dissolved inorganic carbon in the water column without vital effects and small secondary effects of carbonate ion concentrations and pressure (Schmittner et al., 2017).

All age models were updated and synchronized using PaleoDataView (Langner and Mulitza, 2019) and its interface to the Bacon age modeling software (Blaauw and Christen, 2011). Where available, age models are based on planktonic ^{14}C dates, and reservoir age correction is carried out with reservoir ages derived from Butzin et al. (2017). We note that these reservoir age estimates are uncertain, especially for high latitudes (Alves et al., 2019), but they allow the same standard to be applied to records from the same region and result in a consistent dataset. Additionally, surface ocean $\delta^{18}O$ records were regionally compared for consistence and aligned where needed. Cores that lack ^{14}C dating were aligned using the software “BIGMACS” (Bayesian Inference Gaussian process regression for Multiproxy Alignment of Continuous Signals), described in (Lee et al., 2019).

Though different deglacial time slices have been analyzed in the project, here we concentrate on the time slice HS1 that we defined for our study to last from 17.5 to 14.8 ka BP. To account for uncertainties associated with age models and climate transitions (e.g., between the LGM and HS1), the boundaries between time episodes were avoided in our study. Only records covering at least part of the glacial and deglacial time slices (i.e., from the LGM to the YD) are included in the dataset of this study. For quality control, the number of datapoints included from each core for HS1 were plotted and are shown in Figure S1.

4. Results

4.1. Isotope signatures in the eastern North Atlantic basin

During HS1, high benthic $\delta^{13}C_{cc}$ (1.25–0.75‰) indicate the presence of ^{13}C enriched water that occupies the upper 3000 m of the water column at latitudes between 60 °N and 40 °N in the eastern NA basin (Fig. 2c, S2). A strong boundary between ^{13}C enriched (0.5–1.5‰) and ^{13}C depleted (0.0‰) waters to the south is observed between 20 °N and 30 °N. Below 3000 m water depth, the basin is filled with ^{13}C depleted (0.25 to −1‰) waters. In the upper 2000 m, a tongue with a depleted benthic $\delta^{18}O_{cc}$ signature (2.75–3.25‰) is observed between 40 °N and 50 °N (Fig. 2d, S2). The $\delta^{18}O_{cc}$ signal below 2000 m water depth is relatively homogeneous throughout the basin with values between 3.5‰ and 4‰. The $\delta^{18}O_{cc}$ signature does not coincide with that of $\delta^{13}C_{cc}$.

4.2. Western basin

In the Western Atlantic basin, ^{13}C enriched waters (0.5–1.5‰) (Fig. 2a,b, S2) fill the upper 3000 m from 60°N southward. The southernmost extent of this ^{13}C enriched water mass is not well constrained due to the sparsity of data in the South Atlantic, but it seems to extend to ~25°S. This water mass is underlain by ^{13}C depleted waters (0.5 to −1‰). A tongue of waters with a depleted $\delta^{18}O_{cc}$ signature (3–3.5‰) is evident between 60°N and 20°N. It reaches down to about 4000 m at 40° N and shoaling southwards. North of 20°N, the $^{18}O_{cc}$ depleted waters are surrounded by waters with an enriched benthic $^{18}O_{cc}$ signature (3.5–4.5‰). At the equator, a $\delta^{13}C_{cc}$ enrichment to 0–0.25‰ below 3000 m water depth is observed.

4.3. Water mass distribution

4.3.1. HS1 eastern Atlantic water masses

The Irminger and Nordic Seas are filled with deep waters with an enriched ^{18}O and ^{13}C signature, which indicates active deep-water convection in this region and contradicts previous studies suggesting a complete AMOC shut-down (Lund et al., 2015; Rahmsdorf, 2002; Sarnthein et al., 1994; Schmittner and Lund, 2015). Modeling suggests a shut-down AMOC would lead to a $\delta^{13}C$ minimum at 1–2 km depth and 60° N in the North Atlantic due to the accumulation of isotopically-light respired carbon (Schmittner and Lund, 2015), a feature inconsistent with the distribution of $\delta^{13}C_{cc}$ in our HS1 compilation. The HS1 $\delta^{13}C_{cc}$ signature in the eastern North Atlantic basin, shows a depletion of ^{13}C south of 20°N, consistent with previous studies (Duplessy, 1988; Sarnthein et al., 1994). A significant weakening of deepwater formation and AMOC during HS1 and stronger Southern Ocean contributions have been favored as a reason for decreasing $\delta^{13}C_{cc}$ values in the North Atlantic (Duplessy, 1988; Sarnthein et al., 1994; Schmittner and Lund, 2015, and many others), yet already questioned by (Bauch, 2013). More recent studies using combined $\delta^{18}O_{cc}$ and $\delta^{13}C_{cc}$ records from the North Atlantic (Andrews et al., 1999; Campos et al., 2020; Keigwin and Swift, 2017; Repschläger et al., 2015a), show heavy $\delta^{18}O_{cc}$ values during the LGM and HS1 in the deep North Atlantic indicating a northern source of these deep waters (Keigwin and Swift, 2017; Repschläger et al., 2015a) and further questioned the collapsed HS1 AMOC hypothesis.

Data presented here (Fig. 2d) indicate a layer of waters with a depleted $\delta^{18}O_{cc}$ signature in the eastern Atlantic during HS1 between 20°N and 50°N. Yet, these ^{18}O depleted waters are restricted to the upper 2000 m water depth, and seem to reach no further south than 20°N, and thus do not appear to have contributed to deepwater export in the eastern Atlantic. The ^{18}O enriched waters below 3000 m water depth and south of 20°N indicate the existence of another deepwater mass that may have a different origin.

4.3.2. ^{18}O depleted waters

A remarkable tongue of waters with a low $\delta^{18}O_{cc}$ signature enters both the eastern and western Atlantic between 45°N and 20°N. It stays above 2000 m water depth in the eastern basin, whereas in the western North Atlantic it reaches down to 4000 m. These $\delta^{18}O_{cc}$ signatures are not observed south of 20°N. This water mass bears a $^{13}C_{cc}$ enriched signature that is indistinguishable from the water mass signature farther north.

5. Discussion

5.1. Origin of water masses

To better identify the origin and spatial distribution of the different water masses, $\delta^{18}O_{cc}$ and $\delta^{13}C_{cc}$ distributions are plotted along the flow path of the three modern deep- and intermediate water masses, ISOW/NADW, LSW, and MOW (Figs. 1 and 3) (Lherminier et al., 2010; Sarafanov et al., 2012; Schmitz and McCartney, 1993; Xu et al., 2010). Additionally, binned data with 1000-m water-depth bins are used to investigate the spatial extension of the water masses (Fig. 4). Surprisingly, at stations close to the sills to the GIN Seas, $^{18}O_{cc}$ and $^{13}C_{cc}$ enriched signatures are traced (Figs. 3,4,5, S3), our interpretation is that these correspond to the classical ISOW and DSOW waters.

Yet, below 1500 m water depth in the eastern Atlantic basin a ^{13}C depleted, ^{18}O enriched waters are observed and correspond to ENADW. The $\delta^{13}C_{cc}$ depletion may have been caused by several mechanisms: a stronger admixture of stronger ^{13}C depleted (Khatiwala et al., 2019; Martínez-García et al., 2014) southern sourced LDW/AABW to ENADW as previously proposed (Duplessy, 1988; Sarnthein et al., 1994), a general weaker deepwater convection in both the North Atlantic and the Southern Ocean (Zhang et al., 2017) that led to a general increase in residence times of the deepwaters and associated uptake of isotopically-light respired carbon in the ENADW (Crocker et al., 2016; Thornalley et al., 2015) and LDW. The light ISOW $\delta^{13}C_{cc}$ signature in the $\delta^{18}O_{cc}$ vs $\delta^{13}C_{cc}$ cross-plot (Fig. 4) and $\delta^{18}O_{cc}$ signatures similar to AABW in the shallow northern Iceland Basin and the Irminger Sea exclude a southern origin of these waters and indicates that the deepwater filling the abyssal eastern North Atlantic are of Northern origin.

When plotted along the modern NADW flow path, a water mass enriched in $^{18}O_{cc}$ and $^{13}C_{cc}$ can be traced back to the Iceland Sea/Nordic Seas below 1000 m water depth (Fig. 3a and b). Its reconstructed southward flow crosses the Iceland Basin and CGFZ, and seems to be interrupted in the region of the Irminger Sea, Labrador Sea, and the east coast of North America between 50 and 35°N (7000–15,000 km) (Figs. 3 and 4). Within this area, a ^{18}O depleted ^{13}C enriched water mass reaches down to more than 3000 m water depth. This area resembles the area of HS1 meltwater extent reconstructed by the distribution of ice rafted debris (IRD) (Hemming, 2004; Ruddiman, 1977). A potential origin of the ^{18}O depleted water is the relatively warm and saline MOW. Under modern conditions, the ^{18}O depleted, ^{13}C enriched waters sourced from the Mediterranean overflow (Fig. 3e and f, Fig. 4) reach down to 2500 m water depth in the eastern Atlantic basin. Although this is slightly deeper than MOW distribution (Curry et al., 2003), this indicates that $^{18}O_{cc}$ depleted waters in the eastern North Atlantic basin could be affected by MOW. This is also evident from the $\delta^{13}C_{cc}/\delta^{18}O_{cc}$ cross plots (Fig. 5).

In the western North Atlantic basin, the ^{18}O depleted water mass reaches down to 3500 m depth, which is far deeper than its counterpart in the eastern basin (2000 m). The question arises,

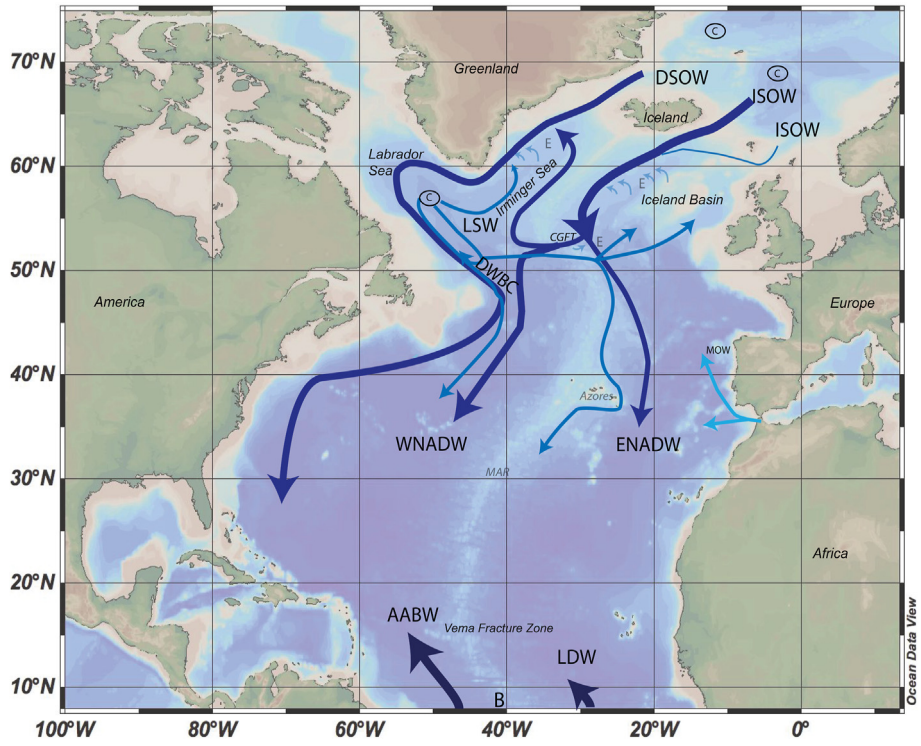

Fig. 1. Map overview on the modern deepwater circulation in the North Atlantic, modified after Repschläger et al. (2015a), based on Schott et al. (2004) supplemented with data of van Sebille et al. (2011) and (van Aken, 2000a); van Aken (2000b); (van Aken, 2001). Abbreviations: ISOW Iceland–Scotland Overflow Water; DSOW Denmark–Strait-Overflow-Water; DWBC Deep Western Boundary Current, LSW Labrador-Sea Water; MOW Mediterranean Overflow Water; ENADW Eastern North Atlantic Deep Water; WNADW Western North Atlantic Deep Water; LDW Lower Deep Water; AABW Antarctic Bottom Water; CGFT Charlie–Gibbs-Fracture-Zone; E Entrainment, © Deepwater convection areas. Map based on Ocean Data View (Schlitzer, 2012).

whether this water mass is affected by MOW or represents an altered DSOW/ISOW or LSW. Along the modern flow path of LSW (Fig. 3), these waters are mainly found along the east coast of North America and the southern tip of Greenland. Data resolution does not allow to prove any admixture of MOW, and densities of modern MOW do not allow these waters to sink below 2000 m. Therefore, we assume that the observed light $\delta^{18}O_{cc}$ in the western North Atlantic basin originates from a western source and not from MOW directly.

A clear boundary between the ^{18}O depleted ^{13}C enriched water mass signature to the north and ^{13}C depleted ^{18}O enriched water to the south is observed at 20°N in the western Atlantic basin below about 2 km depth (Fig. 2). The origin of the ^{13}C depleted and ^{18}O enriched water masses can be traced back to the southernmost sites of our study (Fig. 2a and b, 3a,b), indicating its origin from the Southern Ocean. The extremely light $\delta^{13}C$ signature (Figure S4e, Supplementary Information) is associated with the uptake of respired carbon during the long residence time of the deepwater in the abyssal Southern Ocean and/or an increase in the biological pump in the Southern Ocean, for example, by iron fertilization.

Surprisingly, below 3500 m water depth $\delta^{13}C$ depleted waters from the North and the South are separated by relatively $\delta^{13}C$ enriched waters at the equator (Fig. 2a). Waters below 4000 m at the equator are lighter in its $\delta^{13}C$ signature than the waters to the North of it (Figure S4e). With up to 0.75‰, the signal is statistically significant and may indicate that the abyssal water mass north of the equator originates from the North Atlantic. The boundary is probably formed by well-ventilated mid-depth waters being mixed down to the abyssal ocean at the interface between deep waters of southern and northern origins. Our hypothesis is supported by benthic ^{14}C AMS data compiled by Zhao et al. (2018) that reveal younger ages in the deep North Atlantic than its southern counterpart, in agreement with data and modeling studies for HS1 (Repschläger et al., 2015a) and the LGM (Gebbie, 2014; Keigwin and Swift, 2017; Zhao et al., 2018). Consequently, the existence of northern and southern sources of abyssal waters during HS1 argues against the classical suggestion that southern sourced deep waters filled the entire abyssal ocean during the LGM and HS1 (Curry and Oppo, 2005; Oppo et al., 2018; Rahmsdorf, 2002; Sarnthein et al., 1994).

Based on the above properties and distribution patterns, we distinguish seven different deepwater masses filling the North Atlantic during HS1:

ISOW is characterized by relatively high benthic $\delta^{18}O_{cc}$ and $\delta^{13}C_{cc}$ values. Its formation area is situated in the Nordic Seas and/or Iceland Basin. Its water mass signature is similar to modern ISOW, indicating a deepwater formation process similar to the modern situation. The early disruption of its classical flow path at 50°N in the western Atlantic basin points either to a weak deepwater formation, in agreement with previous studies (Duplessy, 1988; Sarnthein et al., 1994), or to an alteration of ISOW on its southward flow path. The latter would be in agreement with relative strong ISOW formation during HS1 (Crocker et al., 2016), and is discussed in chapter 5.3.

DSOW is characterized by relatively high benthic $\delta^{18}O_{cc}$ and $\delta^{13}C_{cc}$ values and only traceable in the Irminger Basin close to Denmark Strait.

ENADW is characterized by $^{18}O_{cc}$ enriched $^{13}C_{cc}$ intermediate to depleted signatures and fills the eastern North Atlantic basin below 3000 m water depth.

MOW is characterized by benthic $\delta^{18}O_{cc}$ depletion and $\delta^{13}C_{cc}$ enrichment and its flow path corresponds to the classical MOW

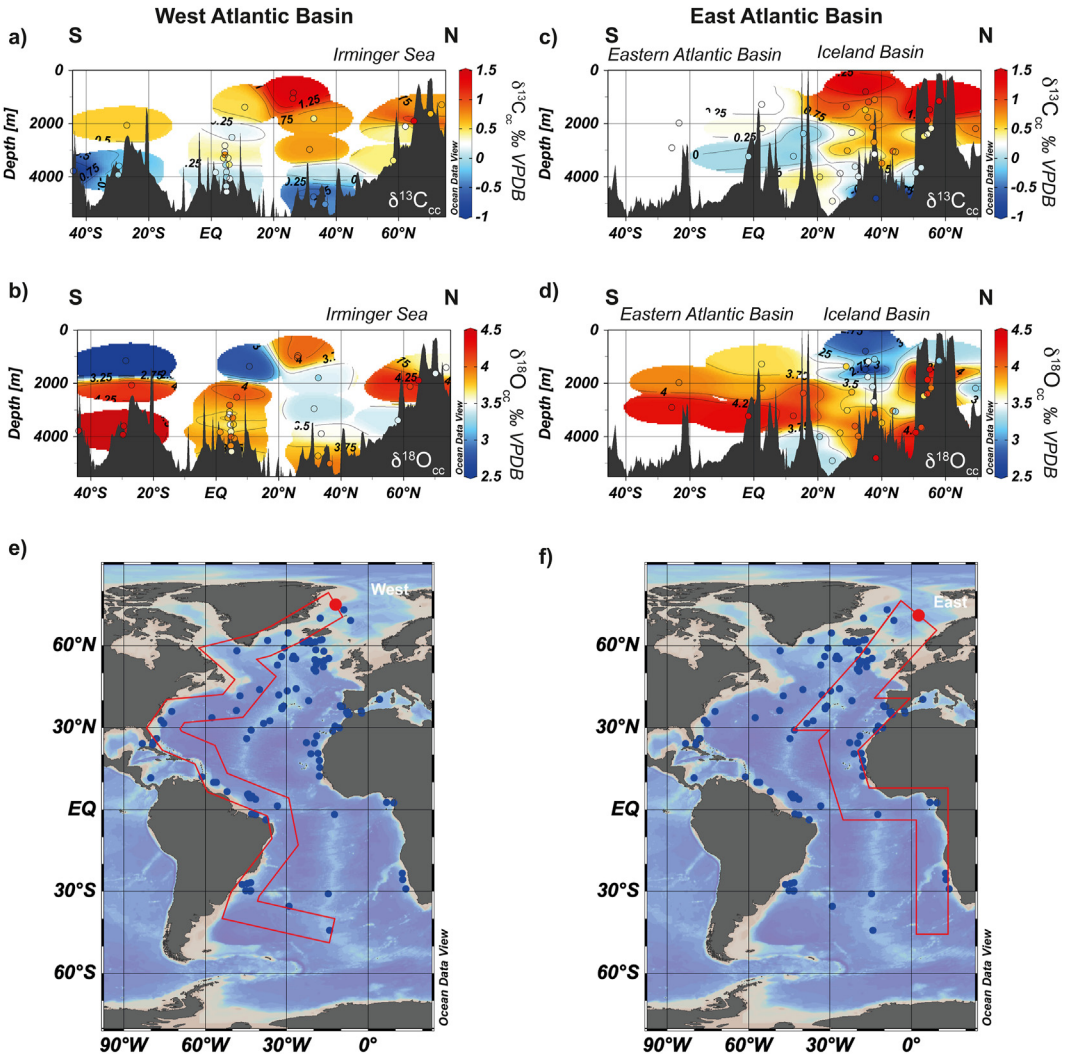

Fig. 2. $\delta^{13}C_{cc}$ (a, c) and $\delta^{18}O_{cc}$ (b, d) sections across the western (a, b) and eastern (c, d) Atlantic for HS1. Panels (e) and (f) show maps indicating the core locations used for both sections.

spreading into the North Atlantic.

HS1-NADW is characterized by low-$\delta^{18}O_{cc}$ high-$\delta^{13}C_{cc}$ benthic signatures and situated in the subtropical to subpolar North Atlantic between 20°N and 50°N. The wide distribution of ^{18}O-depleted signatures below 3000 m water depth (Figs. 2b and 3b) and occupation of the deep western North Atlantic basin, as well as its occurrence at the southern tip of Greenland, argues against its origin from MOW. Though HS1 NADW occupies the space that in modern days is filled with LSW, LSW formation is supposed to have been absent until 7 ka BP (Hoogakker et al., 2011; Kissel et al., 2013; Solignac et al., 2004; Thornalley et al., 2013). Thus, in the following, this water mass is called HS1-NADW. The $\delta^{18}O$ signature of this water mass significantly differs from ISOW signature. Thus, a deepwater formation process different from the Nordic Seas or an alteration of the ISOW must have occurred in the region between 45°N and 50°N, as is discussed in chapter 5.3.

Below 4000 m water depth and to the north of 20°N, the western North Atlantic Basin is filled with LNADW with a $^{13}C_{cc}$-depleted, $^{18}O_{cc}$-enriched (Fig. 2a and b) signature. This water mass probably originated from the north and is poorly ventilated due to weaker abyssal ocean circulation than the mid-depths.

South of the equator, below 2000 m depth, both the eastern and western Atlantic basins are filled with AABW/LDW with high-$\delta^{18}O_{cc}$, low-$\delta^{13}C_{cc}$ signature, which are likely of southern origin (e.g., Oppo et al., 2015; Oppo et al., 2018) and correspond to modern AABW and LDW. They will not be further addressed in this study.

5.2. Water mass formation mechanisms during HS1

5.2.1. Formation of ISOW

Modern ISOW is formed by the cooling of warm saline North Atlantic Current (NAC) waters. Classical circulation patterns for HS1 suggest blocking of the northward warm water transport by a meltwater lens and cessation of subpolar deepwater formation. These scenarios are in contradiction with the $\delta^{18}O$ and $\delta^{13}C$ signatures observed in this study that indicate active deepwater formation in the Iceland Basin during HS1. The latter was previously reported also for HS11 in the Nordic Seas (Bauch, 2013). Though potentially subject to changes in the erosion patterns (Struve et al., 2019), ε_{Nd} and sortable silt records from the Irminger Sea (Crocker et al., 2016 and citations therein) further support the export of deepwater from the Irminger Sea during HS1. Thus, a mechanism needs to be found that can explain northward NAC transport and ISOW formation during HS1.

Despite blocking of the NAC by the meltwater lens and asynchronous warming of the subtropics (Benway et al., 2010), and

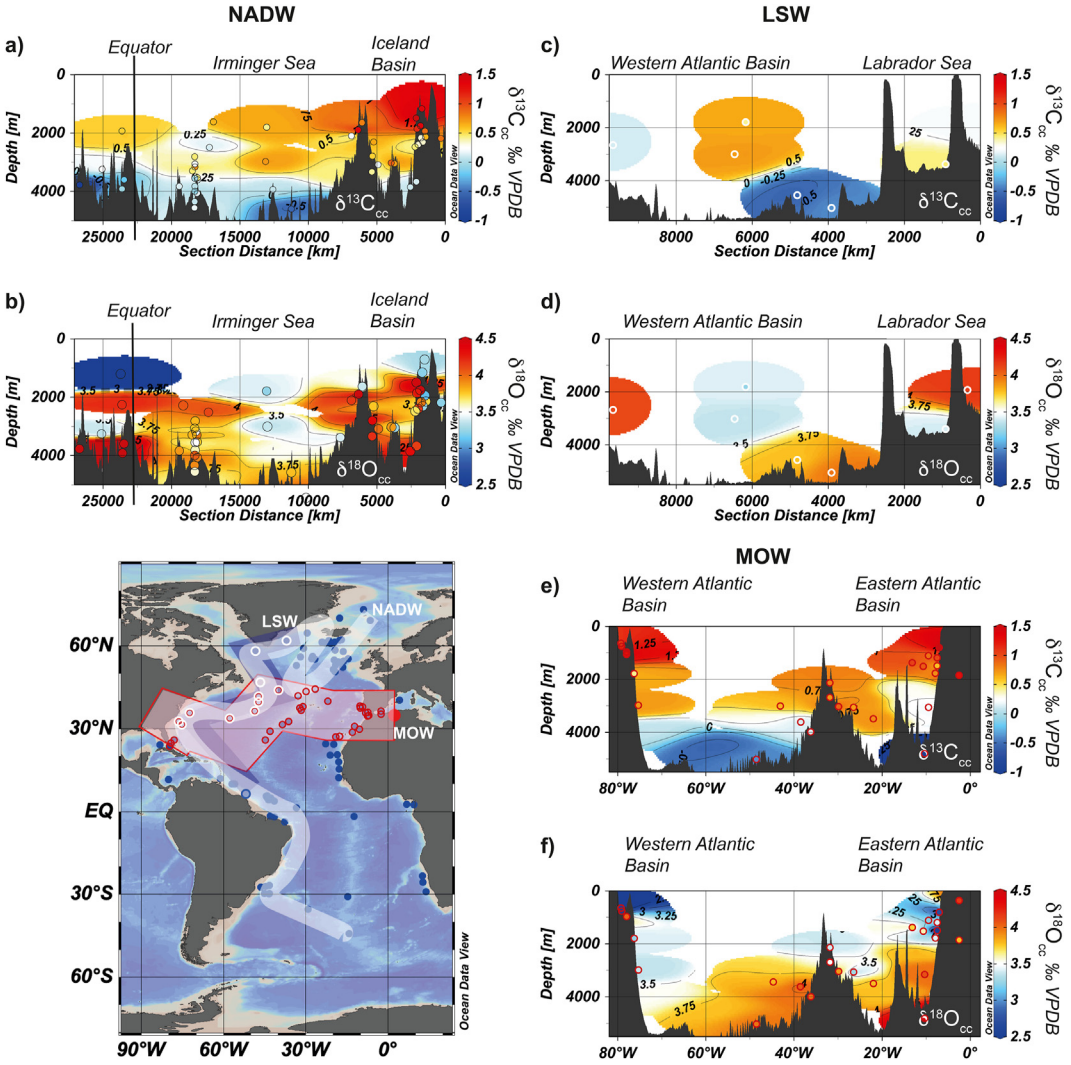

Fig. 3. a) benthic $\delta^{13}C_{cc}$ and b) benthic $\delta^{18}O_{cc}$ distribution during HS1 along the flow path of NADW, c) d) LSW (white circles), and e) f) MOW (red circles).

widespread cooling at the Iberian Margin and subpolar North Atlantic (40–55°N) (Bard et al., 2000; Chapman et al., 2000; Heinrich, 1988; Maslin et al., 1995; Naafs et al., 2011; Penaud et al., 2016; Pérez-Folgado et al., 2003), north of 55°N surface water warming of at least 2 °C between the LGM and HS1 is apparent in Mg/Ca and MAT data from core ODP 980 (Benway et al., 2010) situated at Rockall Plateau, as well as in Mg/Ca SST records of planktonic foraminifera in core RAPID-15–4 P south of Iceland (Thornalley et al., 2011). Mg/Ca records of *G. bulloides* (Peck et al., 2008) indicate strong warming during HS1 and are suggested to be caused by sporadic northward warm water transport with advection of *G. bulloides* from warmer areas (Peck et al., 2008) and is in agreement with studies from the Nordic Seas (Bauch, 2013) and the North Atlantic (Bauch et al., 2000). This warm (and presumably salty) water advection may have fueled sporadic deepwater formation in the subpolar North Atlantic. Yet, the warm NAC waters would need to be transported across the meltwater lens. Two scenarios are possible for the latter: a) surface transport and mixing with the meltwater, and b) subduction of the NAC waters underneath the meltwater, and resurfacing and cooling of the meltwater lens on its transport to the north (Fig. 6). To comprehend this process, analyses of the surface processes including detailed spatial SST and SSS analyses of surface and subsurface dwelling foraminifers would be needed.

5.2.2. Formation of MOW

MOW formation in the Mediterranean may have been increased during HS1 due to higher salinities and regional surface water cooling. Assuming a reduced formation of ISOW during the same time interval, MOW may even have contributed more to the deepwater export than under modern conditions (Bauch, 2013; Rogerson et al., 2010; Schönfeld, 1997; Schönfeld and Zahn, 2000; Voelker et al., 2006). Consequently, MOW may have transported over longer distances and penetrated greater depth in the eastern and western North Atlantic.

5.2.3. Formation of NADW

In the following, we discuss four different mechanisms that may explain the occurrence of the light $\delta^{18}O_{cc}$ signature during HS1 at 1000 to 4,000 m water depths in the western North Atlantic between 20°N and 50°N. As discussed, pure MOW probably can be ruled out as the primary origin for the $\delta^{18}O_{cc}$ depleted water mass signature in the Western Atlantic Basin. The origin of the light $\delta^{18}O_{cc}$ signature can either be admixture of isotopically light waters during active deepwater formation within this area or warming of the deepwater. We first present different mechanisms of NADW

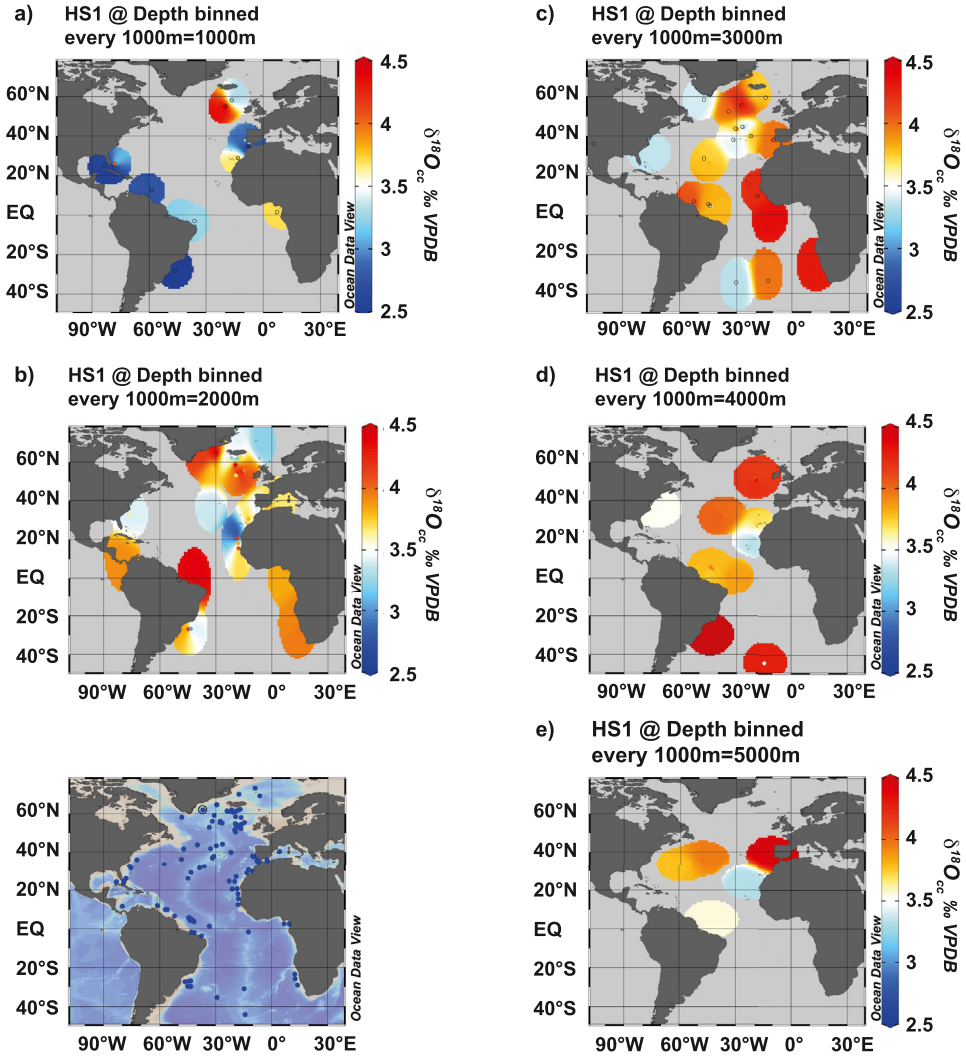

Fig. 4. Regional distribution of benthic $\delta^{18}O_{cc}$ data at 1000 m–5000 m water depth during HS1. Binned depth intervals of 1000 m are used for plotting.

formation and deepwater warming, and then discuss their feasibility based on the $\delta^{18}O_{cc}$ signatures, temperature, salinity, and resulting density.

Mechanism A (Fig. 6a) - convection at the southern edge of meltwater lens: HS1 was associated with a strong cooling of mid-latitudes (Bard et al., 2000; Chapman et al., 2000; Heinrich, 1988; Maslin et al., 1995; Naafs et al., 2011; Penaud et al., 2016; Pérez-Folgado et al., 2003) and an extreme southward displacement of the Arctic Front (e.g. Bard et al., 1987; Eynaud et al., 2009 and citations therein) as well as a southward displacement of the North Atlantic Subtropical Gyre (Repschläger et al., 2015b). Glacial iceberg scours found on the eastern US shelf indicate that the meltwaters from these bergs – potentially also during HS1 – reached as far into the subtropical ocean as the Florida Strait (Hill and Condron, 2014), consequently leading to cooling of that region. Under such cold conditions, strong cooling of the Gulf Stream and NAC waters could have appeared along the southern extension of the meltwater lens, and the southern boundary of the winter sea ice extent (Fig. 7). Cold and strong winds during HS1 could have enhanced such a cooling and eventually have led to deepwater formation. Admixture or entrainment of meltwater into the downwelling water mass during destratification events may have transported the ^{18}O depleted waters into the deep ocean. Although deepwater formation off the coast of the eastern US has not been investigated so far, our proposed open-ocean convection at the southern edge of the meltwater lens (Fig. 7, Mechanism A) is in agreement with reconstructed destratification of the upper water column based on stable oxygen isotope records from different planktonic foraminifera at 40°N during HS1 (Rashid and Boyle, 2007).

Mechanism B (Fig. 7b) - warm polynyas: Warm NAC waters could have been subducted underneath the freshwater and sea ice lens, similar to modern circulation in the Arctic Ocean (Polyakov et al., 2012, and citations therein). Sporadic break-up of sea ice by subsurface warming would lead to the opening of polynyas and cause deepwater convection by cooling of the warm and saline surfacing waters. Similar mechanisms are reported from the Arctic and subpolar North Atlantic (Morales Maqueda et al., 2004) and have been discussed previously (Bauch and Bauch, 2001; Bauch et al., 2001). Presumingly, this process includes entrainment of meltwaters into the newly formed deepwaters, and would lead to a stepwise erosion of the meltwater lens, similar to the mechanism proposed by Krebs and Timmermann (2007) that preconditioned the AMOC resumption at the onset of the Bølling-Allerød.

Mechanism C (Fig. 7c) - cold polynyas: This scenario is similar to modern deepwater formation in the Southern Ocean, i.e., freezing of sea ice and increasing the salinity of the surface waters.

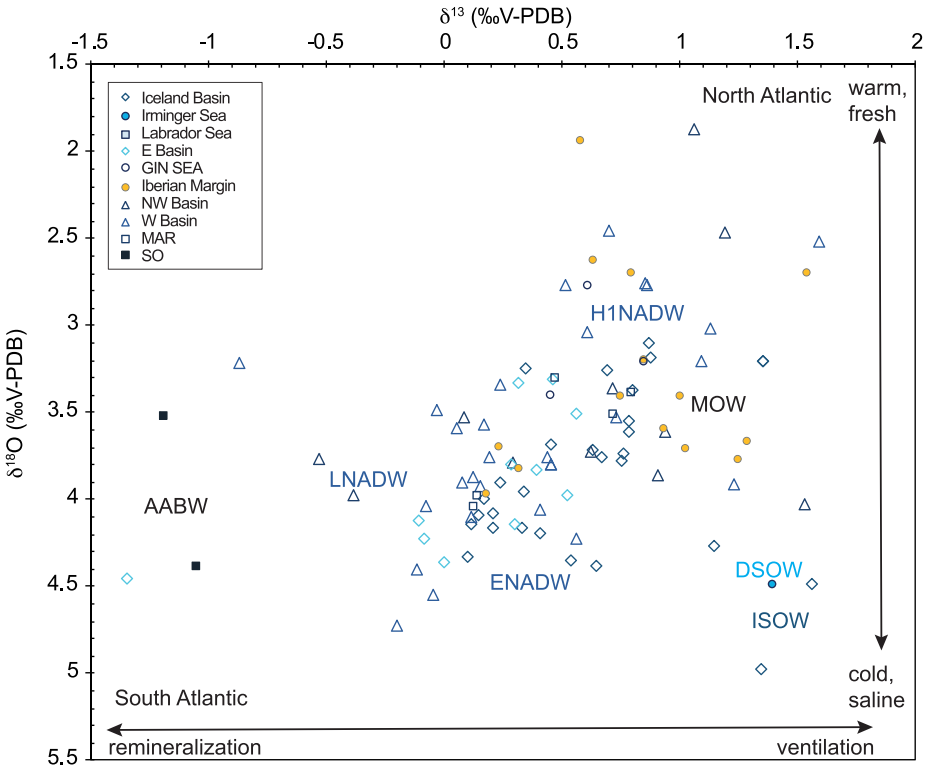

Fig. 5. $\delta^{18}O_{cc}$ versus $\delta^{13}O_{cc}$ cross plots for the dataset for HS1.

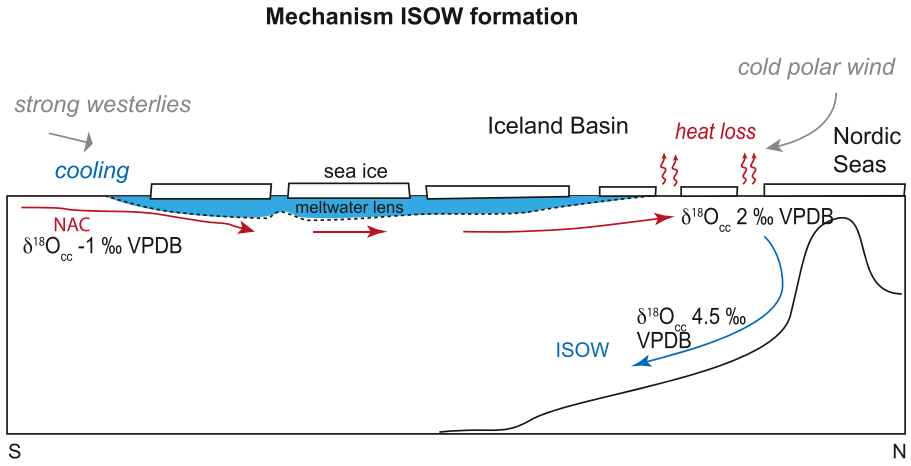

Fig. 6. Mechanism for deepwater formation in the Iceland Basin during HS1 assuming subduction of the NAC underneath the meltwater lens, its northward transport, resurfacing, cooling and convection north of the meltwater lens.

Additional opening of polynyas would lead to heat loss and favor deep water formation by brine water rejection. This scenario is most likely to occur on the Greenland shelf and/or the Labrador Sea, and has previously been proposed (Meland et al., 2008; Waelbroeck et al., 2011) and discussed (Bauch et al., 2001; Bauch and Bauch, 2001).

Mechanism D (Fig. 7d) describes deepwater formation within the Irminger and/or Iceland Basin, its southward transport, and abyssal warming underneath the meltwater lens. This scenario would be consistent with a diffusive heat transport within the water column as published by (de Lavergne et al., 2017). As low $\delta^{18}O$ is mainly occurring underneath the meltwater lid, a connection between both meltwater lid and abyssal warming is likely. The latter may be caused by two different mechanisms: subsurface warming caused by the subduction of NAC waters underneath the meltwater lens, or increased heat transport from enhanced MOW.

5.3. ^{18}O-depleted deep waters-a density paradox?

The signature of low $\delta^{18}O_{cc}$ in the deep Atlantic during HS1 has been reported previously (Campos et al., 2020; Waelbroeck et al., 2001) and is assumed to show the drawdown of the ^{18}O-depleted signal from waters stored in the global ice sheets that are released during the deglaciation into the global ocean. The isotopically light

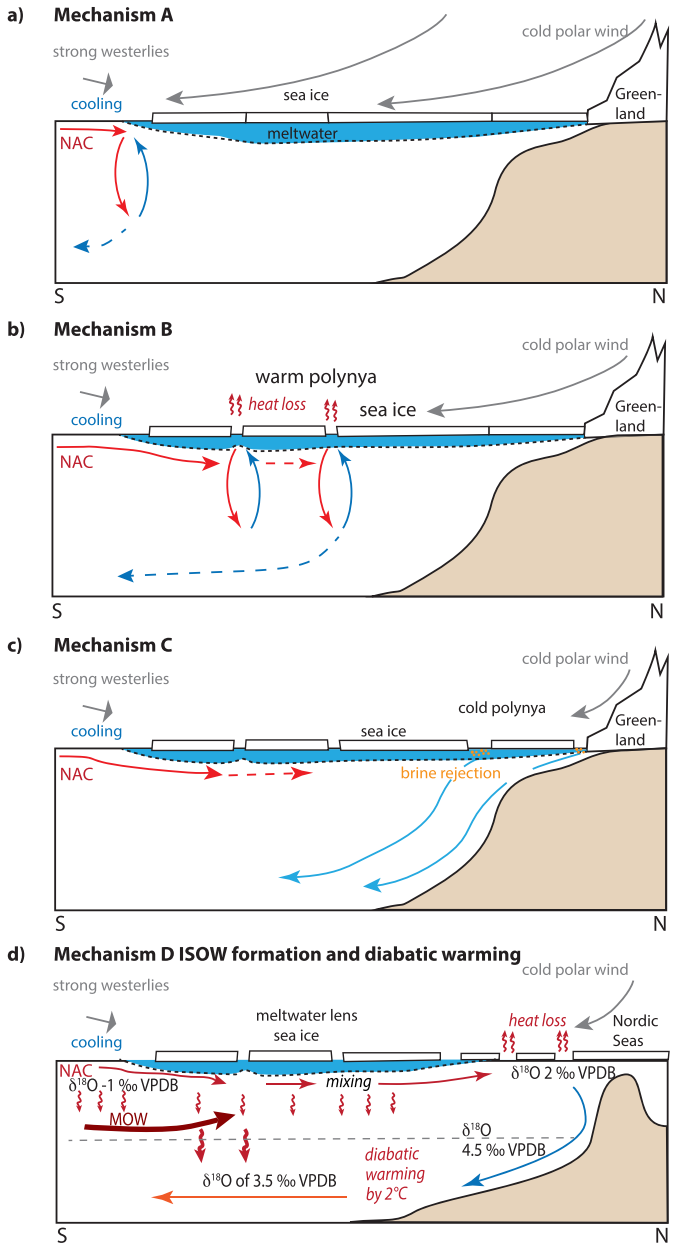

Fig. 7. Four mechanisms for deepwater formation in the subpolar to subtropical North Atlantic during HS1. (a) describes cooling and convection at the southern limit of the meltwater lens; (b) subsurface warm water transport and opening of warm water polynyas; (c) deepwater formation due to the opening of coldwater polynyas and brine rejection; (d) subsurface warm water transport and opening of warm water polynyas and deepwater formation north of the meltwater lens and diabatic heating of the water column beneath the meltwater lens, with major heat contribution from the MOW.

$\delta^{18}O$ signals are caused by the extreme isotopic depletion of the melting ice and resulting fresh water (Vetter et al., 2017). Increased salinity and cooling of these waters would be needed to form waters that are dense enough for deep convection. Both processes increase the $\delta^{18}O$ values, thus preventing the light $\delta^{18}O$ signal from being transported into the deep sea.

The classical explanation for this paradox is deepwater formation by brine rejection. Freezing of sea ice is a process with little isotope fractionation that leaves salt behind in the ocean, thus decoupling $\delta^{18}O$ from salinity. This mechanism illustrated in deepwater formation Scenario C (Fig. 7c) is widely used to explain the deglacial drawdown of the light $\delta^{18}O$ signal during the deglaciation. While explaining the depleted $\delta^{18}O_{cc}$ signature, this concept does not explain deglacial warming and salinity decrease of NADW proposed by Adkins et al. (2002). In the following, we will discuss two different mechanisms that explain the occurrence of $^{18}O_{cc}$ depleted benthic signals under the consideration of deglacial deep ocean temperature and salinity changes: mixing of low $\delta^{18}O$ meltwaters with high $\delta^{18}O$ tropical waters, and abyssal warming of the deepwater.

Mixing of isotopically depleted cold meltwaters and isotopically enriched warm and salty subtropical (NAC) waters is illustrated in Fig. 8 using the $\delta^{18}O_{cc}$ of calcite. The temperature dependence of the $\delta^{18}O$ fractionation in calcite during cooling follows isotope fractionation lines, calculated using the equation of Shackleton (1974). Temperature and isotopic signature of foraminifera for the subtropical water masses was taken from published data from a core (26JPC) situated in the Florida Strait (Schmidt and Lynch-Stieglitz, 2011). For meltwater data core PC04 from the inner Labrador Sea (Gibb et al., 2014) representing the meltwater outburst from Hudson Strait was used. Mixing of about 50% of subtropical waters and 50% of meltwaters and its cooling to deepwater temperatures of 2 °C, as reconstructed for the late HS1 (Cronin et al., 2000; Repschläger et al., 2015a), results in $\delta^{18}O_{cc}$ signatures of 3.5‰ as observed in the western Atlantic basin during HS1 (Fig. 8). Surface temperatures and $\delta^{18}O_{cc}$ data from the subtropical and subpolar North Atlantic are within the range of the anticipated fractionation line. Thus, simple mixing and cooling of surface waters could explain the observed deepwater $\delta^{18}O_{cc}$ signature. Yet, it needs to be tested whether this water mass would still be dense enough to form the observed deepwater masses.

The salinity of the resulting mixed water mass was calculated as follows. For the HS1 meltwater dinocyst-based salinity reconstructions from the inner Labrador Sea in front of Hudson Strait were used (Gibb et al., 2014). Its reconstructed salinities of 31 are in good agreement with modern meltwater signatures from the Hudson Strait (Locarnini et al., 2013). No direct salinity reconstructions exist for the Gulf Stream/NAC waters. Thus, we calculated the latter using the ice volume and Mg/Ca temperature corrected $\delta^{18}O_{sw}$ record of core JPC26 (Schmidt and Lynch-Stieglitz, 2011) using the equations of Fairbanks et al. (1992). To visualize the entire possible range of salinities, we used the regression line for slope waters as well as Sargasso Sea waters. The only existing deepwater salinity reconstructions independent of $\delta^{18}O_{sw}$ were generated from porewaters on a LGM time slice (Adkins et al., 2002). The LGM data represent the saltiest endmember of NADW (Fig. 8b). A water mass mixed from about 50% subtropical and 50% meltwaters would have a salinity between 33.8 and 36. When cooled down to 2.5 °C its density would lie within the range of glacial NADW reconstructed by Adkins et al. (2002).

These results in general indicate the feasibility of deepwater formation with low $\delta^{18}O_{cc}$ signatures by pure mixing of water masses without evoking any brine water formation. Yet, these results highly depend on the assumed $\delta^{18}O$-salinity relationship of the subtropical water masses and have a very high uncertainty. To fully assess the salinity changes involved in this process, independent surface and deepwater salinity reconstructions would be needed.

To test whether NADW was formed independently from ISOW or originates from an altered ISOW or MOW, in the following we discuss different mechanisms that could explain the $\delta^{18}O_{cc}$ signature of foraminifers bathed in ISOW. The $\delta^{18}O_{cc}$ signature of 4.2‰ as observed in the Iceland Basin can be generated by deepwater formation from a mixture of 75% subtropical waters and 25% meltwater (cooling line B) under the assumption of Bottom Water Temperature (BWT) of 2 °C, or by cooling a mixture of 50%

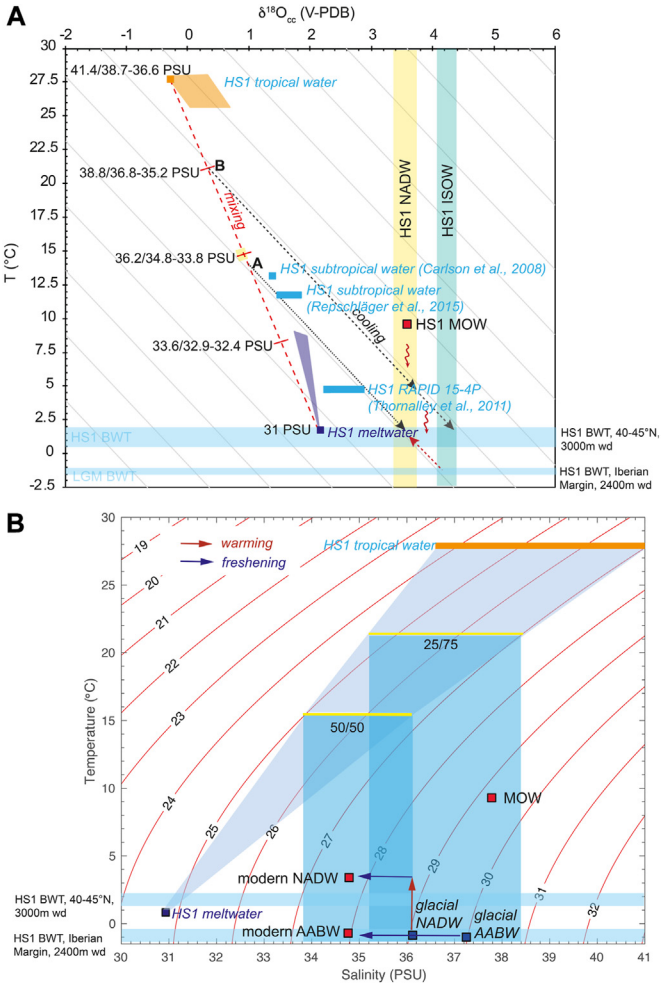

Fig. 8. Mixing of meltwater and subtropical waters as source of the observed deep-water $\delta^{18}O_{cc}$ signature during HS1. (a) $\delta^{18}O_{cc}$ plotted versus water temperature, with the light-yellow vertical shading indicating the observed range of deepwater $\delta^{18}O_{cc}$ data in the deep western Atlantic Basin (NADW) (20–50°N at 1000–4000 m water depth) from this study. The turquoise field indicates $\delta^{18}O_{cc}$ data in the Iceland Basin (ISOW) (1000–3000 m water depth from this study. Grey lines indicate $\delta^{18}O_{cc}$ fractionation lines calculated using the equation of Shackleton (1974). The orange field represents the range for tropical surface waters reported by Carlson et al. (2008) and Schmidt and Lynch-Stieglitz (2011). The violet field indicates surface values reported from the subpolar North Atlantic (e.g., Thornalley et al., 2010; Benway et al., 2010), and the dark blue square indicates the HS1 meltwater signature from the inner Labrador Sea (Gibb et al., 2014). (b) Isolines of potential densities (sigma-theta; orange lines) of different mixtures shown on a T-S diagram. Yellow bars correspond to the crossing point of the cooling lines A and B with the water mass mixing line in plot. Red squares indicate modern NADW, AABW (Adkins et al., 2002) and MOW (Locarnini et al., 2013) signatures. Blue squares indicate HS1 meltwater signature (Gibb et al., 2014), and reconstructed glacial deepwater signatures (Adkins et al., 2002). The orange bar represents the reconstructed T-S range of tropical waters (Schmidt and Lynch-Stieglitz (2011). The horizontal light blue bars in both plots indicates HS1 Bottom Water Temperature (BWT) range reconstructed by Repschläger et al. (2015a) and Skinner and Shackleton (2006), respectively.

subtropical waters and 50% meltwater (cooling line A) to −1.5 °C. Thus, NADW and ISOW during HS1 either originate from the same water mass and only differ in temperatures, or originate from two different deepwater sources that differ in meltwater admixtures. Surface $\delta^{18}O_{cc}$ from the Iceland Basin (Thornalley et al., 2011) better match mixing line A, as well as the average BWT of −0.5 to −1 °C reconstructed from the Iceland Basin (Thornalley et al., 2011) and the Iberian Margin (Skinner and Shackleton, 2006) at 2400 m water depth. Therefore, the $\delta^{18}O_{cc}$ signature of 4‰ can be explained by the cooling of a 50% subtropical and 50% meltwater mixture to the reconstructed temperatures.

5.4. The role of MOW and diabatic heat transport during HS1

The draw-down of isotopically light water to the deep Atlantic can be explained with simple mixing and cooling, as shown above. The reconstructed deepwater warming of 2 °C toward the end of HS1 (Barker et al., 2011; Repschläger et al., 2015a; Skinner and Shackleton, 2006; Thornalley et al., 2015) would lead to a density loss of about 0.2 kg*m^{-3} that argues against a drawdown by active deepwater convection. To keep the density high enough for convection, either additional salt would be needed, or deep ocean warming and increased mixing rates would need to be assumed. MOW with modern salinities of 37.4 could act as a source of salt to the deep water. Yet, under modern conditions, downward mixing of MOW is restricted to the upper 2000 m of the water column. Therefore, stronger vertical mixing of the water column due to heating and or stronger tidal energy dissipation (Wilmes et al., 2019) of the deep ocean would probably be needed (see 5.5).

Three different sources of heat are conceivable: (1) geothermal heating, as has been proposed for the Southern Ocean (Miller et al., 2012), (2) diabatic warming by heat transported downward from the subducted NAC, or (3) from MOW. The distribution pattern of depleted $^{18}O_{cc}$ with a major decrease at intermediate depths argues against (1) geothermal heating at the seafloor. An average heat flux of 116.3 mW*m^{-2} in the North Atlantic region (Bullard and Day, 1961; Davies, 2013) is not sufficient to heat a water column of 3000 m by 2 °C even under the assumption of a complete shutdown of AMOC and stagnation of deepwater flow in the North Atlantic and the a potentially higher geothermal heating at the termination of the LGM because of lower sea level (Lund et al., 2016). (2) Subduction of the NAC underneath the meltwater lens is comparable to the modern situation in the Nordic Seas and Arctic (Polyakov et al., 2012). No modern deepwater warming is reported from this region, therefore, we suppose that warming from the NAC played a subordinate role. (3) Under modern conditions, MOW brings 11 °C warm waters down to a depth of 1,500 m. Therefore, diabatic heat transport from this source to the abyssal ocean may have played a major role in the deepwater warming, especially when considering an MOW strengthening during the later part of this period (Bahr et al., 2014, 2015; Lebreiro et al., 2018; Voelker et al., 2006).

If our hypothesis is correct, and heating resulted from diabatic warming, the deepwater would not have warmed immediately at the beginning of HS1, but would have started sometime later. Indeed, a time delay is also apparent in $\delta^{18}O_{cc}$ time series data, with the $\delta^{18}O_{cc}$ decrease not starting before 16 ka BP (Waelbroeck et al., 2011), yet would need to be tested with benthic bottom water temperature reconstructions.

5.5. The role of vertical mixing

Traditionally, the strengthening of the AMOC after HS1 is explained by a salinity kick-off caused by the onset of the northward transport of warm saline waters, and its cooling and sinking. The production of saline deep waters argues against successive freshening needed to leave the glacial deepwater circulation mode (Adkins et al., 2002). To replace the glacial saline deepwater, a process is required that mixes down freshwaters into the abyssal ocean.

The southern extent of the waters with light $\delta^{18}O_{cc}$ confined to 20 °N indicates a reduced southward transport of NADW and ISOW and has been associated with a weak AMOC in previous studies (e.g., Rahmsdorf, 2002; Sarnthein et al., 1994). This weak AMOC mode probably led to an increased residence time of deepwaters in

the North Atlantic, and increased the proportion of diabatic heat transport (de Lavergne et al., 2017) and diffusive vertical mixing over the meridional mixing component as calculated previously for the South Atlantic (Lund et al., 2011). Increased dissipation of tidal energy may also have contributed to an increase in diapycnal mixing, particularly in the North Atlantic (Wilmes et al., 2019). Such an increased vertical mixing would have led to an increased ventilation that is supported by heavy $\delta^{13}C_{cc}$ signatures. Furthermore, vertical mixing would have favored NADW freshening by downward mixing as well as diabatic warming of the deepwater indicated by light $\delta^{18}O_{cc}$ signatures. This has been shown in a modeling study as asymmetrical warming of the North Atlantic (Zhang et al., 2017), and also explains the deglacial stratification reversal.

5.6. Importance of HS1 in setting the deglacial climate

The sum of our arguments supports Scenario D (Fig. 7d) and explains deepwater formation in HS1. During HS1, tropical warm and saline waters accumulated within the subtropics and were partially exported northward underneath the HS1 meltwater lens. On its northward path, NAC waters entrained overlying meltwaters (about 50%–50% mixing), thereby decreasing its $\delta^{18}O$ signature. In the Irminger/Iceland Basin, NAC waters resurfaced, cooled down, and formed ISOW. The cooling process led to an increase of $\delta^{18}O_{cc}$ in foraminifera, masking the freshening signal of the waters. ISOW slowly propagated into the western Atlantic basin on a flow path similar to modern. In the area between 50°N and 20°N, the deepwater was warmed by diabatic heat transport. The heat originated from MOW as well as warm surface waters that accumulated in the subtropics. The reduction of deepwater flow and thus long residence times favored the deepwater warming and its vertical mixing. This process would have led to a weakening of the salinity driven stratification of the water column, and, at the same time, transport of both heat and freshwater into the abyssal ocean. Consequent weakening of the stratification eventually also allowed deepwater formation Scenarios A and B (Fig. 7), and mixing may have also led to an entrainment of MOW.

The strong vertical mixing and stratification weakening, which is traceable in our dataset by the drawdown of isotopically light $\delta^{18}O$ in wide parts of the North Atlantic, may have set the conditions for the massive deepwater formation during the Bølling-Allerød. This proposed new mechanism shows that the HS1 meltwater outburst is not only an important driver of Southern Ocean upwelling by teleconnection, but also had a direct effect on the reversal of the deepwater stratification in the North Atlantic, which allowed the resumption of the strong AMOC during the BA.

6. Summary and conclusions

The OC3 North Atlantic compilation of epibenthic $\delta^{13}C_{cc}$ and $\delta^{18}O_{cc}$ with improved spatial coverage allows the reconstruction of water mass origin and distribution as well as water mass composition changes along the flow path of the water masses. Distinct patterns of $\delta^{13}C_{cc}$ and $\delta^{18}O_{cc}$ are observed in the deep North Atlantic for HS1 and indicate seven different water masses. ISOW and DSOW originated from a convection cell situated in the Icelandic Basin/Nordic Seas and produced deepwater with a classical heavy $\delta^{13}C$ and $\delta^{18}O$ signature. These waters mainly supplied the eastern and western Atlantic basin at high latitudes. Strong contributions of ^{18}O-depleted and ^{13}C-enriched MOW can be reconstructed for the eastern Atlantic. NADW-like deep waters (HS1-NADW) are situated in the subtropical to subpolar North Atlantic north of 20°N and show distinct high $\delta^{13}C_{cc}$ and low $\delta^{18}O_{cc}$ signatures underneath the HS1 meltwater lens. Its formation may involve deepwater convection underneath and at the boundaries of the meltwater lens as well as diabatic warming of ISOW due to a weakened southward export and thus long residence times. The abyssal North Atlantic below 4000 m probably have been filled with waters of northern origin with a low $\delta^{13}C_{cc}$ and high $\delta^{18}O_{cc}$ signature north of 20°N corresponding to ENADW and LNADW. South of the 20°N, waters with a southern origin prevailed (LDW/AABW).

Enhanced mixing of meltwaters, subtropical waters, and MOW in the upper 3500 m of the water column during long residence times and successive diabatic warming of the deepwaters may explain the drawdown of isotopically light $\delta^{18}O$ and fresh waters into the abyssal North Atlantic that started the salinity reversal of the deep ocean and preconditioned the onset of deepwater convection during the BA. To test the proposed mechanisms, deepwater salinity and temperature reconstructions with proxies independent of oxygen isotope composition would be needed. The new reconstruction also presents a challenge for future modeling studies to reproduce carbon and oxygen isotope distributions during HS1.

Author contribution

Janne Repschläger: project administration, conceptualization, methodology, formal analyses, investigation, resources, writing - original draft, funding acquisition (PAGES) Ning Zhao: Methodology, data curation, software, resources, writing - original draft, Lorraine Lisiecki: Formal analysis, software, writing - review & editing, Devin Rand: Formal analyses, Juan Muglia: methodology, data curation, writing - review & editing, Stefan Mulitza: software, methodology, writing - review & editing, Henning Bauch: resources, writing - review & editing, Andreas Schmittner: project administration, Funding acquisition, writing - review & editing, Olivier Cartapanis: data curation, writing - review & editing, Ralf Schiebel: writing - discussion, review & editing, Gerald Haug: Funding acquisition.

Data availability

All data in PDV file format is uploaded to Pangea and will be made available upon publication. Furthermore, this dataset will be part of the global Pages OC 3 data compilation.

Declaration of competing interest

The authors declare that they have no known competing financial interests or personal relationships that could have appeared to influence the work reported in this paper.

Acknowledgements

The work was supported by the PAGES. AS, JM and OC3 meetings were supported by the National Science Foundation (grants 1634719 and 1924215). OC was funded by the Swiss National Science Foundation (grant PP00P2-144811) and by the Canadian Institute for Advanced Research (CIFAR).

Appendix A. Supplementary data

Supplementary data to this article can be found online at https://doi.org/10.1016/j.quascirev.2021.107145.

References

Abrantes, F., Baas, J., Haflidason, H., Rasmussen, T., Klitgaard, D., Loncaric, N., Gaspar, L., 1998. Sediment fluxes along the northeastern European Margin:

inferring hydrological changes between 20 and 8 kyr. Mar. Geol. 152, 7–23. https://doi.org/10.1016/S0025-3227(98)00062-0.
Abrantes, F.F., Gaspar, L., Helmers, E., Loncaric, N., Monteiro, J., 2018. Geochemical Properties, Stable Isotopes and Foraminifera Abundances in Sediment Cores from the Portuguese Margin Taken during the POSEIDON Cruise PO200/10 in 1993. European North Atlantic Margin (ENAM): Sediment Pathways, Processes and Fluxes. PANGAEA.
Adkins, J.F., 2013. The role of deep ocean circulation in setting glacial climates. Paleoceanography 28, 539–561. https://doi.org/10.1002/palo.20046.
Adkins, J.F., McIntyre, K., Schrag, D.P., 2002. The salinity, temperature, and d18O of the glacial deep ocean. Science 298, 1769–1773. https://doi.org/10.1126/science.1076252.
Alves, E.Q., Macario, K.D., Urrutia, F.P., Cardoso, R.P., Bronk Ramsey, C., 2019. Accounting for the marine reservoir effect in radiocarbon calibration. Quat. Sci. Rev. 209, 129–138. https://doi.org/10.1016/j.quascirev.2019.02.013.
Andrews, J.T., Keigwin, L., Hall, F., Jennings Anne, E., 1999. Abrupt deglaciation events and Holocene palaeoceanography from high-resolution cores, Cartwright Saddle, Labrador Shelf, Canada. J. Quat. Sci. 14, 383–397. https://doi.org/10.1002/(SICI)1099-1417(199908)14:5<383::AID-JQS464>3.0.CO;2-J.
Bahr, A., Jiménez-Espejo, F.J., Kolasinac, N., Grunert, P., Hernández-Molina, F.J., Röhl, U., Voelker, A.H.L., Escutia, C., Stow, D.A.V., Hodell, D., Alvarez-Zarikian, C.A., 2014. Deciphering bottom current velocity and paleoclimate signals from contourite deposits in the Gulf of Cádiz during the last 140 kyr: an inorganic geochemical approach. G-cubed 15, 3145–3160. https://doi.org/10.1002/2014GC005356.
Bahr, A., Kaboth, S., Jiménez-Espejo, F.J., Sierro, F.J., Voelker, A.H.L., Lourens, L., Röhl, U., Reichart, G.J., Escutia, C., Hernández-Molina, F.J., Pross, J., Friedrich, O., 2015. Persistent monsoonal forcing of mediterranean outflow water dynamics during the late pleistocene. Geology 43, 951–954. https://doi.org/10.1130/G37013.1.
Balmer, S., Sarnthein, M., 2018. Glacial-to-deglacial changes in North Atlantic meltwater advection and deep-water formation – centennial-to-millennial-scale 14C records from the Azores plateau. Geochem. Cosmochim. Acta 236, 399–415. https://doi.org/10.1016/j.gca.2018.03.001.
Balmer, S., Sarnthein, M., Mudelsee, M., Grootes Pieter, M., 2016. Refined modeling and 14C plateau tuning reveal consistent patterns of glacial and deglacial 14C reservoir ages of surface waters in low-latitude Atlantic. Paleoceanography 31, 1030–1040. https://doi.org/10.1002/2016PA002953.
Bard, E., Arnold, M., Maurice, P., Duprat, J., Moyes, J., Duplessy, J.-C., 1987. Retreat velocity of the North Atlantic polar front during the last deglaciation determined by 14C accelerator mass spectrometry. Nature 328, 791–794. https://doi.org/10.1038/328791a0.
Bard, E., Rostek, F., Turon, J.-L., Gendreau, S., 2000. Hydrological impact of Heinrich events in the subtropical northeast atlantic. Science 289, 1321–1324. https://doi.org/10.1126/science.289.5483.1321.uring OIS 5e in the Western Mediterranean. Journal on Geomorphology 110, 231–235.
Baringer, M.O.N., Price, J.F., 1997. Mixing and spreading of the mediterranean outflow. J. Phys. Oceanogr. 27, 1654–1677. https://doi.org/10.1175/1520-0485(1997)027<1654:MASOTM>2.0.CO;2.
Barker, S., Knorr, G., Edwards, R.L., Parrenin, F., Putnam, A.E., Skinner, L.C., Wolff, E., Ziegler, M., 2011. 800,000 Years of abrupt climate variability. Science 334, 347.
Bauch, D., Bauch, H.A., 2001. Last glacial benthic foraminiferal δ18O anomalies in the polar North Atlantic: a modern analogue evaluation. J. Geophys. Res.: Oceans 106, 9135–9143. https://doi.org/10.1029/1999JC000164.
Bauch, H.A., 2013. Interglacial climates and the Atlantic meridional overturning circulation: is there an Arctic controversy? Quat. Sci. Rev. 63, 1–22. https://doi.org/10.1016/j.quascirev.2012.11.023.
Bauch, H.A., Erlenkeuser, H., Spielhagen, R.F., Struck, U., Matthiessen, J., Thiede, J., Heinemeier, J., 2001. A multiproxy reconstruction of the evolution of deep and surface waters in the subarctic Nordic seas over the last 30,000yr. Quat. Sci. Rev. 20, 659–678. https://doi.org/10.1016/S0277-3791(00)00098-6.
Bauch, H.A., Erlenkeuser, H., Jung, S.J.A., Thiede, J., 2000. Surface and deep water changes in the subpolar North Atlantic during Termination II and the Last Interglaciation. Paleoceanography 15, 76–84. https://doi.org/10.1029/1998PA000343.
Benway, H.M., McManus, J.F., Oppo, D.W., Cullen, J.L., 2010. Hydrographic changes in the eastern subpolar North Atlantic during the last deglaciation. Quat. Sci. Rev. 29, 3336–3345. https://doi.org/10.1016/j.palaeo.2003.12.014.
Bertram, C.J., Elderfield, H., Shackleton, N.J., MacDonald, J.A., 1995. Cadmium/calcium and carbon isotope reconstructions of the glacial northeast Atlantic Ocean. Paleoceanography 10, 563–578. https://doi.org/10.1029/94PA03058.
Beveridge, N.A.S., Elderfield, H., Shackleton, N.J., 1995. Deep thermohaline circulation in the low-latitude atlantic during the last glacial. Paleoceanography 10, 643–660. https://doi.org/10.1029/94PA03353.
Bickert, T., Mackensen, A., 2004. Last Glacial to Holocene Changes in South Atlantic Deep Water Circulation, the South Atlantic in the Late Quaternary. Springer Berlin Heidelberg, pp. 671–693.
Blaauw, M., Christen, J.A., 2011. Flexible paleoclimate age-depth models using an autoregressive gamma process. Bayesian Anal 6, 457–474. https://doi.org/10.1214/11-BA618.
Böhm, E., Lippold, J., Gutjahr, M., Frank, M., Blaser, P., Antz, B., Fohlmeister, J., Frank, N., Andersen, M.B., Deininger, M., 2015. Strong and deep Atlantic meridional overturning circulation during the last glacial cycle. Nature 517, 73–76. https://doi.org/10.1038/nature14059.
Boyle, E.A., Keigwin, L.D., 1985. Comparison of Atlantic and Pacific paleochemical records for the last 215,000 years: changes in deep ocean circulation and chemical inventories. Earth Planet Sci. Lett. 76, 135–150.
Broecker, W.S., 1994. Massive iceberg discharges as triggers for global climate change. Nature 372, 421–424. https://doi.org/10.1038/372421a0.
Bullard, E.C., Day, A., 1961. The flow of heat through the floor of the Atlantic Ocean. Geophys. J. Roy. Astron. Soc. 4, 282–292. https://doi.org/10.1111/j.1365-246X.1961.tb06820.x.
Butzin, M., Köhler, P., Lohmann, G., 2017. Marine radiocarbon reservoir age simulations for the past 50,000 years. Geophys. Res. Lett. 44, 8473–8480. https://doi.org/10.1002/2017GL074688.
Cacho, I., Shackleton, N., Elderfield, H., Sierro, F.J., Grimalt, J.O., 2006. Glacial rapid variability in deep-water temperature and δ18O from the Western Mediterranean Sea. Quat. Sci. Rev. 25, 3294–3311. https://doi.org/10.1016/j.quascirev.2006.10.004.
Came, R.E., Oppo, D.W., Curry, W.B., Lynch-Stieglitz, J., 2008. Deglacial variability in the surface return flow of the Atlantic meridional overturning circulation. Paleoceanography 23, PA1217. https://doi.org/10.1029/2007pa001450.
Campos, M.C., Chiessi, C.M., Venancio, I.M., Pinho, T.M.L., Crivellari, S., Kuhnert, H., Schmiedl, G., Díaz, R.A., Albuquerque, A.L.S., Portilho-Ramos, R.C., Bahr, A., Mulitza, S., 2020. Constraining millennial-scale changes in northern component water ventilation in the western tropical South Atlantic. Paleoceanography and Paleoclimatology 35. https://doi.org/10.1029/2020PA003876 e2020PA003876.
Carlson, A.E., Oppo, D.W., Came, R.E., LeGrande, A.N., Keigwin, L.D., Curry, W.B., 2008. Subtropical Atlantic salinity variability and Atlantic meridional circulation during the last deglaciation. Geology 36, 991–994. https://doi.org/10.1130/g25080a.1.
Chafik, L., Hátún, H., Kjellsson, J., Larsen, K.M.H., Rossby, T., Berx, B., 2020. Discovery of an unrecognized pathway carrying overflow waters toward the Faroe Bank Channel. Nat. Commun. 11, 3721. https://doi.org/10.1038/s41467-020-17426-8.
Chapman, M., Shackleton, N.J., Duplessy, J.-C., 2000. Sea surface temperature variability during the last glacial-intreglcial cycle: assessing the magnitude and pattern of climatic change in the North Atlantic. Paleogeography, Paleoclimatology, Paleoecology 157, 1–25. https://doi.org/10.1016/S0031-0182(99)00168-6.
Chi, J., Mienert, J.r., 2003. Age Model of Sediment Core GIK23416-4. PANGAEA.
Colin, C., Frank, N., Copard, K., Douville, E., 2010. Neodymium isotopic composition of deep-sea corals from the NE Atlantic: implications for past hydrological changes during the Holocene. Quat. Sci. Rev. 29, 2509–2517. https://doi.org/10.1016/j.palaeo.2003.12.014.
Collins, J.A., Schefusz, E., Heslop, D., Mulitza, S., Prange, M., Zabel, M., Tjallingii, R., Dokken, T.M., Huang, E., Mackensen, A., Schulz, M., Tian, J., Zarriess, M., Wefer, G., 2010. Interhemispheric symmetry of the tropical African rainbelt over the past 23,000 years. Nat. Geosci. 4, 42–45. https://doi.org/10.1038/NGEO1039.
Crocker, A.J., Chalk, T.B., Bailey, I., Spencer, M.R., Gutjahr, M., Foster, G.L., Wilson, P.A., 2016. Geochemical response of the mid-depth Northeast Atlantic Ocean to freshwater input during Heinrich events 1 to 4. Quat. Sci. Rev. 151, 236–254. https://doi.org/10.1016/j.quascirev.2016.08.035.
Cronin, T.M., Dwyer, G.S., Baker, P.A., Rodriguez-Lazaro, J., DeMartino, D.M., 2000. Orbital and suborbital variability in North Atlantic bottom water temperature obtained from deep-sea ostracod Mg/Ca ratios. Palaeogeogr. Palaeoclimatol. Palaeoecol. 162, 45–57. https://doi.org/10.1016/S0031-0182(00)00104-8.
Curry, R., Dickson, B., Yashayaev, I., 2003. A change in the freshwater balance of the Atlantic Ocean over the past four decades. Nature 426, 826–829. https://doi.org/10.1038/nature02206.
Curry, W.B., Duplessy, J.C., Labeyrie, L.D., Shackleton, N.J., 1988. Changes in the distribution of δ13C of deep water ΣCO2 between the last glaciation and the Holocene. Paleoceanography 3, 317–341. https://doi.org/10.1029/PA003i003p00317.
Curry, W.B., Marchitto, T.M., McManus, J.F., Oppo, D.W., Laarkamp, K.L., 1999. Millennial-scale Changes in Ventilation of the Thermocline, Intermediate, and Deep Waters of the Glacial North Atlantic, Mechanisms of Global Climate Change at Millennial Time Scales, pp. 59–76.
Curry, W.B., Oppo, D.W., 1997. Synchronous, high-frequency oscillations in tropical sea surface temperatures and north atlantic deep water production during the last glacial cycle. Paleoceanography 12, 1–14. https://doi.org/10.1029/96PA02413.
Curry, W.B., Oppo, D.W., 2005. Glacial water mass geometry and the distribution of δ13C of ΣCO2 in the western Atlantic Ocean. Paleoceanography 20, PA1017. https://doi.org/10.1029/2004PA001021.
Davies, J.H., 2013. Global map of solid Earth surface heat flow. G-cubed 14, 4608–4622. https://doi.org/10.1002/ggge.20271.
de Lavergne, C., Madec, G., Roquet, F., Holmes, R.M., McDougall, T.J., 2017. Abyssal ocean overturning shaped by seafloor distribution. Nature 551, 181–186. https://doi.org/10.1038/nature24472.
Denton, G.H., Anderson, R.F., Toggweiler, J.R., Edwards, R.L., Schaefer, J.M., Putnam, A.E., 2010. The last glacial termination. Science 328, 1652–1656. https://doi.org/10.1126/science.1184119.
Dickson, A.J., Beer, C.J., Dempsey, C., Maslin, M.A., Bendle, J.A., McClymont, E.L., Pancost, R.D., 2009. Oceanic forcing of the marine isotope stage 11 interglacial. Nat. Geosci. 2, 428–433. https://doi.org/10.1038/ngeo527.
Duplessy, J.-C., 1982. North Atlantic deep water circulation during the last climate cycle. Bull. Inst. Geol. Bassin Aquitaine 31, 379–391.
Duplessy, J.-C., Labeyrie, L., Waelbroeck, C., 2002. Constraints on the ocean oxygen isotopic enrichment between the last glacial maximum and the Holocene: paleoceanographic implications. Quat. Sci. Rev. 21, 315–330. https://doi.org/

10.1016/S0277-3791(01)00107-X.
Duplessy, J.-C., Shackleton, N.J., Matthews, R.K., Prell, W., Ruddiman, W.F., Caralp, M.I., Hendy, C.H., 1984. 13C Record of benthic foraminifera in the last interglacial ocean: implications for the carbon cycle and the global deep water circulation. Quat. Res. 21, 225–243. https://doi.org/10.1016/S0921-8181(01)00074-1.
Duplessy, J.C., 1988. Deepwater source variations during the last climatic cycle and their impact on global deepwater circulation. Paleoceanography 3, 343–360. https://doi.org/10.1029/PA003i003p00343.
Duplessy, J.C., Moyes, J., Pujol, C., 1980. Deep water formation in the North Atlantic Ocean during the last ice age. Nature 286, 479–482. https://doi.org/10.1038/286479a0.
Elliot, M., 2017. Paleoclimate data from sediment core SU90-24, Irminger basin. PANGAEA.
Elmore, A.C., Wright, J.D., 2011. North Atlantic deep water and climate variability during the younger dryas cold period. Geology 39, 107–110. https://doi.org/10.1130/g31376.1.
Elmore, A.C., Wright, J.D., Southon, J., 2015. Continued meltwater influence on north atlantic deep water instabilities during the early Holocene. Mar. Geol. 360, 17–24. https://doi.org/10.1016/j.margeo.2014.11.015.
Eynaud, F., de Abreu, L., Voelker, A., Schönfeld, J., Salgueiro, E., Turon, J.-L., Penaud, A., Toucanne, S., Naughton, F., Sánchez Goñi, M.F., Malaizé, B., Cacho, I., 2009. Position of the Polar Front along the western Iberian margin during key cold episodes of the last 45 ka. G-cubed 10, Q07U05. https://doi.org/10.1029/2009gc002398.
Ezat, M.M., Rasmussen, T.L., Skinner, L.C., Zamelczyk, K., 2019. Deep ocean 14C ventilation age reconstructions from the Arctic Mediterranean reassessed. Earth Planet Sci. Lett. 518, 67–75. https://doi.org/10.1016/j.epsl.2019.04.027.
Fairbanks, R.G., Charles, C.D., Wright, J.D., 1992. Origin of global meltwater pulses. In: Taylor, R.E., Long, A., Kra, R.S. (Eds.), Radiocarbon after Four Decades. Springer New York, New York, NY, pp. 473–500.
Faure, V., Speer, K., 2005. Labrador Sea water circulation in the northern North Atlantic ocean. Deep Sea Res. Part II Top. Stud. Oceanogr. 52, 565–581. https://doi.org/10.1016/j.dsr2.2004.12.004.
Feldmeijer, W., Metcalfe, B., Scussolini, P., Arthur, K., 2013. The effect of chemical pretreatment of sediment upon foraminiferal-based proxies. G-cubed 14, 3996–4014. https://doi.org/10.1002/ggge.20233.
Ferrari, R., Jansen, M.F., Adkins, J.F., Burke, A., Stewart, A.L., Thompson, A.F., 2014. Antarctic sea ice control on ocean circulation in present and glacial climates. Proc. Natl. Acad. Sci. Unit. States Am. 111, 8753. https://doi.org/10.1073/pnas.1323922111.
Fink, H.G., Wienberg, C., De Pol-Holz, R., Wintersteller, P., Hebbeln, D., 2013. Cold-water coral growth in the alboran sea related to high productivity during the late pleistocene and Holocene. Mar. Geol. 339, 71–82. https://doi.org/10.1016/j.margeo.2013.04.009.
Fischer, J., Karstensen, J., Zantopp, R., Visbeck, M., Biastoch, A., Behrens, E., Böning, C.W., Quadfasel, D., Jochumsen, K., Valdimarsson, H., Jónsson, S., Bacon, S., Holliday, N.P., Dye, S., Rhein, M., Mertens, C., 2015. Intra-seasonal variability of the DWBC in the western subpolar North Atlantic. Prog. Oceanogr. 132, 233–249. https://doi.org/10.1016/j.pocean.2014.04.002.
Fischer, J., Schott, F.A., Dengler, M., 2004. Boundary circulation at the exit of the Labrador Sea. J. Phys. Oceanogr. 34, 1548–1570. https://doi.org/10.1175/1520-0485(2004)034<1548:BCATEO>2.0.CO;2.
Fontanier, C., Mackensen, A., Jorissen, F., Anschutz, P., Licari, L., Griveaud, C., 2006. Stable oxygen and carbon isotopes of live benthic foraminifera from the Bay of Biscay: microhabitat impact and seasonal variability. Mar. Micropaleontol. 58, 159–183. https://doi.org/10.1016/j.marmicro.2005.09.004.
Freudenthal, T., Meggers, H., Henderiks, J., Kuhlmann, H., Moreno, A., Wefer, G., 2002. Upwelling intensity and filament activity off Morocco during the last 250,000 years. Deep Sea Res. Part II Top. Stud. Oceanogr. 49, 3655–3674. https://doi.org/10.1016/S0967-0645(02)00101-7.
Frigola, J., Moreno, A., Cacho, I., Canals, M., Sierro, F.J., Flores, J.A., Grimalt, J.O., 2008. Evidence of abrupt changes in Western Mediterranean Deep Water circulation during the last 50kyr: a high-resolution marine record from the Balearic Sea. Quat. Int. 181, 88–104. https://doi.org/10.1016/j.quaint.2007.06.016.
Ganopolski, A., Rahmstorf, S., 2001. Rapid changes of glacial climate simulated in a coupled climate model. Nature 409, 153–158. https://doi.org/10.1038/35051500.
Gebbie, G., 2014. How much did glacial North Atlantic water shoal? Paleoceanography 29, 190–209. https://doi.org/10.1002/2013PA002557.
Gersonde, R., Abelmann, A., Brathauer, U., Becquey, S., Bianchi, C., Cortese, G., Grobe, H., Kuhn, G., Niebler, H.S., Segl, M., Sieger, R., Zielinski, U., Fütterer, D.K., 2003. Last glacial sea surface temperatures and sea-ice extent in the Southern Ocean (Atlantic-Indian sector): a multiproxy approach. Paleoceanography 18, 1061. https://doi.org/10.1029/2002pa000809.
Gibb, O.T., Hillaire-Marcel, C., de Vernal, A., 2014. Oceanographic regimes in the northwest Labrador Sea since Marine Isotope Stage 3 based on dinocyst and stable isotope proxy records. Quat. Sci. Rev. 92, 269–279. https://doi.org/10.1016/j.quascirev.2013.12.010.
Hagen, S., Keigwin, L.D., NOAA, 2002. Blake Outer Ridge Stable Isotope and Carbonate Data. Hagen, S. and L.D. Keigwin. 2005. IGBP PAGES/World Data Center for Paleoclimatology, Data Contribution Series # 2005–026. NOAA/NCDC Paleoclimatology Program, Boulder CO, USA.
Hagen, S., Keigwin, L.D., 2017. Stable Isotope Record of Foraminifera from ODP Site 172-1059. PANGAEA.
Hansen, B., Húsgarð Larsen, K.M., Hátún, H., Østerhus, S., 2016. A stable Faroe Bank channel overflow 1995–2015. Ocean Sci. 12, 1205–1220. https://doi.org/10.5194/os-12-1205-2016.
Hansen, B., Østerhus, S., 2000. North Atlantic–Nordic seas exchanges. Prog. Oceanogr. 45, 109–208. https://doi.org/10.1016/S0079-6611(99)00052-X.
Haskins, R.K., Oliver, K.I.C., Jackson, L.C., Drijfhout, S.S., Wood, R.A., 2019. Explaining asymmetry between weakening and recovery of the AMOC in a coupled climate model. Clim. Dynam. 53, 67–79. https://doi.org/10.1007/s00382-018-4570-z.
Heinrich, H., 1988. Origin and consequences of cyclic ice rafting in the Northeast Atlantic Ocean during the past 130,000 years. Quat. Res. 29, 142–152. https://doi.org/10.1016/0033-5894(88)90057-9.
Hemming, S.R., 2004. Heinrich events: massive late Pleistocene detritus layers of the North Atlantic and their global climate imprint. Rev. Geophys. 42, RG1005. https://doi.org/10.1029/2003rg000128.
Hill, J.C., Condron, A., 2014. Subtropical iceberg scours and meltwater routing in the deglacial western North Atlantic. Nature Geosci advance online publication. https://doi.org/10.1038/ngeo2267. http://www.nature.com/ngeo/journal/vaop/ncurrent/abs/ngeo2267.html#supplementary-information.
Hillaire-Marcel, C., Vernal, A.d., Lucotte, M., Mucci, A., 1994. The Labrador Sea during the late quaternary: introduction. Can. J. Earth Sci. 31, 1–4. https://doi.org/10.1139/e94-001.
Hodell, D.A., Charles, C.D., Curtis, J.H., Mortyn, P.G., Ninnemann, U.S., Venz, K.A., 2003. Data report: oxygen isotope stratigraphy of ODP Leg 177 Sites 1088, 1089, 1090, 1093, and 1094. In: Gersonde, R., Hodell, D.A., Blum, P. (Eds.), Proc. ODP, Sci. Results. Ocean Drilling Program), College Station, TX, pp. 1–26.
Hoffman, J.L., Lund, D.C., 2012. Refining the stable isotope budget for Antarctic Bottom Water: new foraminiferal data from the abyssal southwest Atlantic. Paleoceanography 27. https://doi.org/10.1029/2011PA002216.
Hoogakker, B.A.A., Chapman, M.R., McCave, I.N., Hillaire-Marcel, C., Ellison, C.R.W., Hall, I.R., Telford, R.J., 2011. Dynamics of north atlantic deep water masses during the Holocene. Paleoceanography 26, PA4214. https://doi.org/10.1029/2011PA002155.
Hoogakker, B.A.A., Elderfield, H., Schmiedl, G., McCave, I.N., Rickaby, R.E.M., 2015. Glacial-interglacial changes in bottom-water oxygen content on the Portuguese margin. Nat. Geosci. 8, 40–43. https://doi.org/10.1038/ngeo2317. http://www.nature.com/ngeo/journal/v8/n1/abs/ngeo2317.html#supplementary-information.
Howe, J.N.W., Huang, K.-F., Oppo, D.W., Chiessi, C.M., Mulitza, S., Blusztajn, J., Piotrowski, A.M., 2018. Similar mid-depth atlantic water mass provenance during the last glacial maximum and Heinrich stadial 1. Earth Planet Sci. Lett. 490, 51–61. https://doi.org/10.1016/j.epsl.2018.03.006.
Howe, J.N.W., Piotrowski, A.M., Hu, R., Bory, A., 2017. Reconstruction of east–west deep water exchange in the low latitude Atlantic Ocean over the past 25,000 years. Earth Planet Sci. Lett. 458, 327–336. https://doi.org/10.1016/j.epsl.2016.10.048.
Hüls, C.M., 1999. Millennial-scale SST Variability as Inferred from Planktonic Foraminiferal Census Counts in the Western Subtropical Atlantic. GEOMAR. Christian-Albrechts-Universität, Kiel, p. 123.
Jansen, E., Veum, T., 1990. Evidence for two-step deglaciation and its impact on North Atlantic deep-water circulation. Nature 343, 612–616. https://doi.org/10.1038/343612a0.
Jonkers, L., Cartapanis, O., Langner, M., McKay, N., Mulitza, S., Strack, A., Kucera, M., 2020. Integrating palaeoclimate time series with rich metadata for uncertainty modelling: strategy and documentation of the PalMod 130k marine palaeoclimate data synthesis. Earth Syst. Sci. Data 12, 1053–1081. https://doi.org/10.5194/essd-12-1053-2020.
Jonkers, L., Zahn, R., Thomas, A., Henderson, G., Abouchami, W., François, R., Masque, P., Hall, I.R., Bickert, T., 2015. Deep circulation changes in the central South Atlantic during the past 145 kyrs reflected in a combined 231Pa/230Th, Neodymium isotope and benthic δC13 record. Earth Planet Sci. Lett. 419, 14–21. https://doi.org/10.1016/j.epsl.2015.03.004.
Jung, S.J.A., 1996. Wassermassenaustausch zwischen NE-Atlantik und Nordmeer während der letzten 300.000/80.000 Jahre im Abbild stabiler 0- und C-Isotope, Berichte aus dem Sonderforschungsbereich 313, Veränderungen der Umwelt - Der Nördliche Nordatlantik. Christian-Albrechts-Universität zu Kiel, Kiel, Germany, pp. 1–154.
Keigwin, L., Jones, G.A., 1994. Western North Atlantic evidence for millenial-scale changes in ocean circulation and climate. Journal of Geophysical Reseach 99 (12), 397. https://doi.org/10.1029/94JC00525, 312,410.
Keigwin, L.D., 2004. Radiocarbon and stable isotope constraints on last glacial maximum and younger dryas ventilation in the Western North atlantic. Paleoceanography 19, PA4012. https://doi.org/10.1029/2004pa001029.
Keigwin, L.D., Jones, G.A., Lehman, S.J., Boyle, E.A., 1991. Deglacial meltwater discharge, North Atlantic Deep Circulation, and abrupt climate change. J. Geophys. Res.: Oceans 96, 16811–16826. https://doi.org/10.1029/91JC01624.
Keigwin, L.D., Lehman, S.J., 1994. Deep circulation change linked to HEINRICH event 1 and younger dryas in a middepth North Atlantic core. Paleoceanography 9, 185–194. https://doi.org/10.1029/94PA00032.
Keigwin, L.D., Schlegel, M.A., 2002. Ocean ventilation and sedimentation since the glacial maximum at 3 km in the western North Atlantic. G-cubed 3, 1034. https://doi.org/10.1029/2001gc000283.
Keigwin, L.D., Swift, S.A., 2017. Carbon isotope evidence for a northern source of deep water in the glacial western North Atlantic. Proc. Natl. Acad. Sci. Unit. States Am. 114, 2831–2835. https://doi.org/10.1073/pnas.1614693114.
Khatiwala, S., Schmittner, A., Muglia, J., 2019. Air-sea disequilibrium enhances ocean

carbon storage during glacial periods. Science Advances 5, eaaw4981. https://doi.org/10.1126/sciadv.aaw4981.
Kiefer, T., 1998. Produktivität und Temperaturen im subtropischen Nordatlantik: zyklische und abrupte Veränderungen im späten Quartär, Berichte - Reports, Geologisch-Paläontologisches Institut und Museum, Christian-Albrechts-Universität, Kiel. Geologisch-Paläontologisches Institut und Museum, Christian-Albrechts-Universität, Kiel, Kiel, Germany, pp. 1–127.
Kissel, C., Van Toer, A., Laj, C., Cortijo, E., Michel, E., 2013. Variations in the strength of the north atlantic bottom water during Holocene. Earth Planet Sci. Lett. 369–370, 248–259. https://doi.org/10.1016/j.epsl.2013.03.042.
Knorr, G., Lohmann, G., 2003. Southern Ocean origin for the resumption of Atlantic thermohaline circulation during deglaciation. Nature 424, 532–536. https://doi.org/10.1038/nature01855.
Knorr, G., Lohmann, G., 2007. Rapid transitions in the Atlantic thermohaline circulation triggered by global warming and meltwater during the last deglaciation. G-cubed 8, Q12006. https://doi.org/10.1029/2007GC001604.
Krebs, U., Timmermann, A., 2007. Fast advective recovery of the Atlantic meridional overturning circulation after a Heinrich event. Paleoceanography 22, PA1220. https://doi.org/10.1029/2005PA001259.
Kwon, E.Y., Hain, M.P., Sigman, D.M., Galbraith, E.D., Sarmiento, J.L., Toggweiler, J.R., 2012. North Atlantic ventilation of "southern-sourced" deep water in the glacial ocean. Paleoceanography 27. https://doi.org/10.1029/2011PA002211.
Labeyrie, L., Leclaire, H., Waelbroeck, C., Cortijo, E., Duplessy, J.-C., Vidal, L., Elliot, M., Le Coat, B., Auffret, G., 1999. Temporal variability of the surface and deep waters of the north west Atlantic Ocean at orbital and millenial scales. Mechanisms of Global Climate Change at Millennial Time Scales 77–98.
Labeyrie, L., Vidal, L., Cortijo, E., Paterne, M., Arnold, M., Duplessy, J.C., Vautravers, M., Labracherie, M., Duprat, J., Turon, J.L., Grousset, F., van Weering, T., Eglinton, G., Elderfield, H., Whitfield, M., Williams, P.J.L.B., 1995. Surface and deep hydrology of the Northern Atlantic Ocean during the past 150000 years. Phil. Trans. Roy. Soc. Lond. B Biol. Sci. 348, 255–264. https://doi.org/10.1098/rstb.1995.0067.
Labeyrie, L., Waelbroeck, C., Cortijo, E., Michel, E., Duplessy, J.-C., 2005. Changes in deep water hydrology during the Last Deglaciation. C. R. Geoscience 337, 919–927. https://doi.org/10.1016/j.crte.2005.05.010.
Labeyrie, L.D., 1996. Quaternary Paleoceanography: Unpublished Stable Isotope Records, IGBP PAGES/World Data Center for Paleoclimatology Data Contribution Series #1996-036. NOAA/NGDC Paleoclimatology Program, Boulder. Colorado, USA.
Labeyrie, L.D., Duplessy, J.-C., Duprat, J., Juillet-Leclerc, A., Moyes, J., Michel, E., Kallel, N., Shackleton, N.J., 1992. Changes in the vertical structure of the North Atlantic Ocean between glacial and modern times. Quat. Sci. Rev. 11, 401–413. https://doi.org/10.1016/0277-3791(92)90022-Z.
Langner, M., Mulitza, S., 2019. Technical note: PaleoDataView – a software toolbox for the collection, homogenization and visualization of marine proxy data. Clim. Past 15, 2067–2072. https://doi.org/10.5194/cp-15-2067-2019.
Lebreiro, S.M., Antón, L., Reguera, M.I., Marzocchi, A., 2018. Paleoceanographic and climatic implications of a new Mediterranean Outflow branch in the southern Gulf of Cadiz. Quat. Sci. Rev. 197, 92–111. https://doi.org/10.1016/j.quascirev.2018.07.036.
Lebreiro, S.M., Voelker, A.H.L., Vizcaino, A., Abrantes, F.G., Alt-Epping, U., Jung, S., Thouveny, N., Gràcia, E., 2009. Sediment instability on the Portuguese continental margin under abrupt glacial climate changes (last 60-0 kyr). Quat. Sci. Rev. 28, 3211–3223. https://doi.org/10.1016/j.quascirev.2009.08.007.
Lee, T., Lisiecki, L., Rand, D., Gebbie, G., Lawrence, C., 2019. A Multiple Continuous Signal Alignment Algorithm with Gaussian Process Profiles and an Application to Paleoceanography (arXiv: Applications).
Lherminier, P., Mercier, H., Huck, T., Gourcuff, C., Perez, F.F., Morin, P., Sarafanov, A., Falina, A., 2010. The atlantic meridional overturning circulation and the subpolar gyre observed at the A25-OVIDE section in june 2002 and 2004. Deep Sea Res. Oceanogr. Res. Pap. 57, 1374–1391.
Little, M.G., Schneider, R.R., Kroon, D., Price, B., Bickert, T., Wefer, G., 1997. Rapid palaeoceanographic changes in the Benguela Upwelling System for the last 160,000 years as indicated by abundances of planktonic foraminifera. Palaeogeogr. Palaeoclimatol. Palaeoecol. 130, 135–161. https://doi.org/10.1016/S0031-0182(96)00136-8.
Liu, Z., Otto-Bliesner, B.L., He, F., Brady, E.C., Tomas, R., Clark, P.U., Carlson, A.E., Lynch-Stieglitz, J., Curry, W., Brook, E., Erickson, D., Jacob, R., Kutzbach, J., Cheng, J., 2009. Transient simulation of last deglaciation with a new mechanism for bolling-allerod warming. Science 325, 310–314. https://doi.org/10.1126/science.1171041.
Locarnini, R.A., Mishonov, A.V., Antonov, J.I., Boyer, T.P., Garcia, H.E., Baranova, O.K., Zweng, M.M., Paver, C.R., Reagan, J.R., Johnson, D.R., Hamilton, M., Seidov, D.V., 2013. World ocean atlas 2013. In: NOAA Atlas NESDIS, 73 Volume 1. S. Levitus, Temperature, p. 40.
Lozier, M.S., Stewart, N.M., 2008. On the temporally varying northward penetration of mediterranean overflow water and eastward penetration of Labrador Sea water. J. Phys. Oceanogr. 38, 2097–2103. https://doi.org/10.1175/2008JPO3908.1.
Lund, D.C., Adkins, J.F., Ferrari, R., 2011. Abyssal atlantic circulation during the last glacial maximum: constraining the ratio between transport and vertical mixing. Paleoceanography 26, PA1213. https://doi.org/10.1029/2010pa001938.
Lund, D.C., Asimow, P.D., Farley, K.A., Rooney, T.O., Seeley, E., Jackson, E.W., Durham, Z.M., 2016. Enhanced East Pacific Rise hydrothermal activity during the last two glacial terminations. Science 351, 478. https://doi.org/10.1126/science.aad4296.
Lund, D.C., Tessin, A.C., Hoffman, J.L., Schmittner, A., 2015. Southwest Atlantic watermass evolution during the last deglaciation. Paleoceanography. https://doi.org/10.1002/2014PA002657, 2014PA002657.
Lynch-Stieglitz, J., 2017. The atlantic meridional overturning circulation and abrupt climate change. Annual Review of Marine Science 9, 83–104. https://doi.org/10.1146/annurev-marine-010816-060415.
Lynch-Stieglitz, J., Adkins, J.F., Curry, W.B., Dokken, T., Hall, I.R., Herguera, J.C., Hirschi, J.J.-M., Ivanova, E.V., Kissel, C., Marchal, O., Marchitto, T.M., McCave, I.N., McManus, J.F., Mulitza, S., Ninnemann, U., Peeters, F., Yu, E.-F., Zahn, R., 2007. Atlantic meridional overturning circulation during the last glacial maximum. Science 316, 66–69. https://doi.org/10.1126/science.1137127.
Lynch-Stieglitz, J., Currey, W., Slowey, N., 1999. A geostrophic transport estimate for the Florida Current from oxygen isotope composition of benthic foraminifera. Paleoceanography 14, 360–373.
Lynch-Stieglitz, J., Schmidt, M.W., Curry, W.B., 2011. Evidence from the Florida straits for younger dryas Ocean Circulation changes. Paleoceanography 26, PA1205. https://doi.org/10.1029/2010pa002032.
Lynch-Stieglitz, J., Schmidt, M.W., Gene Henry, L., Curry, W.B., Skinner, L.C., Mulitza, S., Zhang, R., Chang, P., 2014. Muted change in Atlantic overturning circulation over some glacial-aged Heinrich events. Nat. Geosci. 7, 144–150. https://doi.org/10.1038/ngeo2045. http://www.nature.com/ngeo/journal/v7/n2/abs/ngeo2045.html#supplementary-information.
Mackensen, A., 2001. Last glacial maximum deep-water circulation in the subantarctic eastern Atlantic Ocean. AGU Fall Meeting Abstracts 1, 10.
Macrander, A., Send, U., Valdimarsson, H., Jónsson, S., Käse, R.H., 2005. Interannual changes in the overflow from the nordic seas into the Atlantic Ocean through Denmark strait. Geophys. Res. Lett. 32, L06606. https://doi.org/10.1029/2004GL021463.
Manighetti, B., McCave, I.N., Maslin, M., Shackleton, N.J., 1995. Chronology for climate change: developing age models for the biogeochemical ocean flux study cores. Paleoceanography 10, 513–525. https://doi.org/10.1029/94PA03062.
Marchitto, T.M., Curry, W.B., Lynch-Stieglitz, J., Bryan, S.P., Cobb, K.M., Lund, D.C., 2014. Improved oxygen isotope temperature calibrations for cosmopolitan benthic foraminifera. Geochem. Cosmochim. Acta 130, 1–11. https://doi.org/10.1016/j.gca.2013.12.034.
Marshall, J., Schott, F., 1999. Open-ocean convection: observations, theory, and models. Rev. Geophys. 37, 1–64.
Marshall, J., Speer, K., 2012. Closure of the meridional overturning circulation through Southern Ocean upwelling. Nat. Geosci. 5, 171–180.
Martínez-García, A., Sigman, D.M., Ren, H., Anderson, R.F., Straub, M., Hodell, D.A., Jaccard, S.L., Eglinton, T.I., Haug, G.H., 2014. Iron fertilization of the subantarctic ocean during the last ice age. Science 343, 1347–1350. https://doi.org/10.1126/science.1246848.
Maslin, M.A., Shackleton, N.J., Pflaumann, U., 1995. Surface water temperature, salinity, and density changes in the northeast atlantic during the last 45,000 Years: Heinrich events, deep water formation, and climatic rebounds. Paleoceanography 10, 527–544. https://doi.org/10.1029/94pa03040.
McManus, J.F., Francois, R., Gherardi, J.M., Keigwin, L.D., Brown-Leger, S., 2004. Collapse and rapid resumption of Atlantic meridional circulation linked to deglacial climate changes. Nature 428, 834–837. https://doi.org/10.1038/nature02494.
Mead, G.A., Hodell, D.A., Cielsielski, P.F., 1993. Late Eocene to Oligocene vertical isotopic gradients in the South Atlantic: implications for warm saline deep water. In: Kennett, J.P., Warnke, D. (Eds.), The Antarctic Paleoenvironment: A Perspective on Global Change. Am. Geophys. Union, A.R.S., The Antarctic Paleoenvironment: A Perspective on Global Change., vol. 60, pp. 27–48.
Meland, M.Y., Dokken, T.M., Jansen, E., Hevroy, K., 2008. Water mass properties and exchange between the Nordic seas and the northern North Atlantic during the period 23-6 ka: benthic oxygen isotopic evidence. Paleoceanography 23, 19. https://doi.org/10.1029/2007pa001416. Pa1210.
Members, C.P., 1976. The surface of the ice-age earth. Science 191, 1131. https://doi.org/10.1126/science.191.4232.1131.
Members, C.P., 2004. Radiocarbon Age Determinations on Sediment Core V25-59. PANGAEA.
Menviel, L., Spence, P., Yu, J., Chamberlain, M.A., Matear, R.J., Meissner, K.J., England, M.H., 2018. Southern Hemisphere westerlies as a driver of the early deglacial atmospheric CO2 rise. Nat. Commun. 9, 2503. https://doi.org/10.1038/s41467-018-04876-4.
Middleton, J.L., Langmuir, C.H., Mukhopadhyay, S., McManus, J.F., Mitrovica, J.X., 2016. Hydrothermal iron flux variability following rapid sea level changes. Geophys. Res. Lett. 43, 3848–3856. https://doi.org/10.1002/2016GL068408.
Middleton, J.L., Mukhopadhyay, S., Langmuir, C.H., McManus, J.F., Huybers, P.J., 2018. Millennial-scale variations in dustiness recorded in Mid-Atlantic sediments from 0 to 70 ka. Earth Planet Sci. Lett. 482, 12–22. https://doi.org/10.1016/j.epsl.2017.10.034.
Miller, M.D., Adkins, J.F., Menemenlis, D., Schodlok, M.P., 2012. The role of ocean cooling in setting glacial southern source bottom water salinity. Paleoceanography 27. https://doi.org/10.1029/2012PA002297.
Millo, C., 2005. Primary and Secondary Signals of Variations in the Denmark Strait Overflow over the Last Glacial Cycle. Institute of Geosciences Christian-Albrechts-University Kiel, Kiel, p. 75.
Millo, C., Sarnthein, M., Voelker, A., Erlenkeuser, H., 2008. Variability of the Denmark Strait Overflow during the last glacial maximum. Boreas 35, 50–60. https://doi.org/10.1111/j.1502-3885.2006.tb01112.x.
Morales Maqueda, M.A., Willmott, A.J., Biggs, N.R.T., 2004. Polynya dynamics: a

review of observations and modeling. Rev. Geophys. 42. https://doi.org/10.1029/2002RG000116.
Muglia, J., Schmittner, A., 2021. Glacial atlantic meridional overturning circulation: strength vs depth. Quat. Sci. Rev. 257, 106844. https://doi.org/10.1016/j.quascirev.2021.106844.
Muglia, J., Skinner, L.C., Schmittner, A., 2018. Weak overturning circulation and high Southern Ocean nutrient utilization maximized glacial ocean carbon. Earth Planet Sci. Lett. 496, 47–56. https://doi.org/10.1016/j.epsl.2018.05.038.
Mulitza, S., Chiessi, C.M., Schefuß, E., Lippold, J., Wichmann, D., Antz, B., Mackensen, A., Paul, A., Prange, M., Rehfeld, K., Werner, M., Bickert, T., Frank, N., Kuhnert, H., Lynch-Stieglitz, J., Portilho-Ramos, R.C., Sawakuchi, A.O., Schulz, M., Schwenk, T., Tiedemann, R., Vahlenkamp, M., Zhang, Y., 2017. Synchronous and proportional deglacial changes in Atlantic meridional overturning and northeast Brazilian precipitation. Paleoceanography 32, 622–633. https://doi.org/10.1002/2017PA003084.
Mulitza, S., Prange, M., Stuut, J.-B., Zabel, M., von Dobeneck, T., Itambi, A.C., Nizou, J., Schulz, M., Wefer, G., 2008. Sahel megadroughts triggered by glacial slowdowns of Atlantic meridional overturning. Paleoceanography 23, PA4206. https://doi.org/10.1029/2008pa001637.
Naafs, B.D.A., Hefter, J., Ferretti, P., Stein, R., Haug, G.H., 2011. Sea surface temperatures did not control the first occurrence of Hudson Strait Heinrich Events during MIS 16. Paleoceanography 26, PA4201. https://doi.org/10.1029/2011pa002135.
Naafs, B.D.A., Hefter, J., Grützner, J., Stein, R., 2013. Warming of surface waters in the mid-latitude North Atlantic during Heinrich events. Paleoceanography 28, 153–163. https://doi.org/10.1029/2012pa002354.
Nam, S.-I., 1997. Late Quaternary glacial history and paleoceanographic reconstructions along the East Greenland continental margin: Evidence from high-resolution records of stable isotopes and ice-rafted debris (Spätquartäre Vereisungsgeschichte und paläozeanographische Rekonstruktionen am ostgrönlandischen Kontinentalrand), Berichte zur Polarforschung = Reports on Polar Research. Alfred-Wegener-Institut für Polar- und Meeresforschung, Bremerhaven, Germany, pp. 1–257.
Oppo, D.W., Curry, W.B., McManus, J.F., 2015. What do benthic δ13C and δ18O data tell us about Atlantic circulation during Heinrich Stadial 1? Paleoceanography 30. https://doi.org/10.1002/2014PA002667, 2014PA002667.
Oppo, D.W., Fairbanks, R.G., 1990. Atlantic Ocean thermohaline circulation of the last 150,000 years: relationship to climate and atmospheric CO2. Paleoceanography 5, 277–288. https://doi.org/10.1029/PA005i003p00277.
Oppo, D.W., Gebbie, G., Huang, K.-F., Curry, W.B., Marchitto, T.M., Pietro, K.R., 2018. Data constraints on glacial atlantic water mass geometry and properties. Paleoceanography and Paleoclimatology 33, 1013–1034. https://doi.org/10.1029/2018PA003408.
Oppo, D.W., Horowitz, M., 2000. Glacial deep water geometry: south Atlantic benthic foraminiferal Cd/Ca and δ13C evidence. Paleoceanography 15, 147–160. https://doi.org/10.1029/1999PA000436.
Oppo, D.W., Lehman, S.J., 1993. Mid-depth circulation of the subpolar North atlantic during the last glacial maximum. Science 259, 1148–1152. https://doi.org/10.1126/science.259.5098.1148.
Oppo, D.W., Lehman, S.J., 1995. Suborbital timescale variability of north atlantic deep water during the past 200,000 years. Paleoceanography 10, 901–910. https://doi.org/10.1029/95PA02089.
Oppo, D.W., McManus, J.F., Cullen, J.L., 2006. Evolution and demise of the last interglacial warmth in the subpolar North atlantic. Quat. Sci. Rev. 25, 3268–3277. https://doi.org/10.1016/j.quascirev.2006.07.006.
Ostermann, D.R., Curry, W.B., 2000. Calibration of stable isotopic data: an enriched δ18O standard used for source gas mixing detection and correction. Paleoceanography 15, 353–360. https://doi.org/10.1029/1999PA000411.
Peck, V.L., Hall, I.R., Zahn, R., Elderfield, H., 2008. Millennial-scale surface and subsurface paleothermometry from the northeast Atlantic, 55–8 ka BP. Paleoceanography 23, PA3221. https://doi.org/10.1029/2008pa001631.
Penaud, A., Eynaud, F., Voelker, A.H.L., Turon, J.L., 2016. Palaeohydrological changes over the last 50 ky in the central Gulf of Cadiz: complex forcing mechanisms mixing multi-scale processes. Biogeosciences 13, 5357–5377. https://doi.org/10.5194/bg-13-5357-2016.
Pérez-Folgado, M., Sierro, F.J., Flores, J.A., Cacho, I., Grimalt, J.O., Zahn, R., Shackleton, N., 2003. Western Mediterranean planktonic foraminifera events and millennial climatic variability during the last 70 kyr. Mar. Micropaleontol. 48, 49–70. https://doi.org/10.1016/S0377-8398(02)00160-3.
Pichevin, L., Martinez, P., Bertrand, P., Schneider, R., Giraudeau, J., Emeis, K., 2005. Nitrogen cycling on the Namibian shelf and slope over the last two climatic cycles: local and global forcings. Paleoceanography 20. https://doi.org/10.1029/2004PA001001.
Pickart, R.S., Spall, M.A., Ribergaard, M.H., Moore, G.K., Milliff, R.F., 2003. Deep convection in the Irminger Sea forced by the Greenland tip jet. Nature 424, 152–156.
Piotrowski, A.M., Galy, A., Nicholl, J.A.L., Roberts, N., Wilson, D.J., Clegg, J.A., Yu, J., 2012. Reconstructing deglacial North and South Atlantic deep water sourcing using foraminiferal Nd isotopes. Earth Planet Sci. Lett. 357–358, 289–297.
Piotrowski, A.M., Goldstein, S.L., R, H.S., Fairbanks, R.G., Zylberberg, D.R., 2008. Oscillating glacial northern and southern deep water formation from combined neodymium and carbon isotopes. Earth Planet Sci. Lett. 272, 394–405. https://doi.org/10.1016/j.epsl.2008.05.011.
Polyakov, I.V., Pnyushkov, A.V., Timokhov, L.A., 2012. Warming of the intermediate atlantic water of the Arctic Ocean in the 2000s. J. Clim. 25, 8362–8370. https://doi.org/10.1175/JCLI-D-12-00266.1.
Praetorius, S.K., McManus, J.F., Oppo, D.W., Curry, W.B., 2008. Episodic reductions in bottom-water currents since the last ice age. Nat. Geosci. 1, 449–452. http://www.nature.com/ngeo/journal/v1/n7/suppinfo/ngeo227_S1.html.
Rahmsdorf, S., 2002. Ocean circulation and climate during the past 120000 years. Nature 419, 207–214.
Rahmstorf, S., 2002. Ocean circulation and climate during the past 120,000 years. Nature 419, 207–214. https://doi.org/10.1038/nature01090.
Rashid, H., Boyle, E.A., 2007. Mixed-layer deepening during Heinrich events: a multi-planktonic foraminiferal d18O approach. Science 318, 439–441. https://doi.org/10.1126/science.1146138.
Repschläger, J., Weinelt, M., Andersen, N., Garbe-Schönberg, D., Schneider, R., 2015a. Northern source for deglacial and Holocene deepwater composition changes in the eastern North Atlantic basin. Earth Planet Sci. Lett. 425, 256–267. https://doi.org/10.1016/j.epsl.2015.05.009.
Repschläger, J., Weinelt, M., Kinkel, H., Andersen, N., Garbe-Schönberg, D., Schwab, C., 2015b. Response of the subtropical North Atlantic surface hydrography on deglacial and Holocene AMOC changes. Paleoceanography 30. https://doi.org/10.1002/2014pa002637.
Richter, T., 1998. Sedimentary Fluxes at the Mid-atlantic Ridge - Sediment Sources, Accumulation Rates, and Geochemical Characterisation. GEOMAR Report, GEOMAR Research Center for Marine Geosciences. Christian Albrechts University in Kiel, p. 173.
Rickaby, R.E.M., Elderfield, H., 2005. Evidence from the high-latitude North Atlantic for variations in Antarctic Intermediate water flow during the last deglaciation. G-cubed 6, Q05001. https://doi.org/10.1029/2004gc000858.
Roberts, J., Gottschalk, J., Skinner, L.C., Peck, V.L., Kender, S., Elderfield, H., Waelbroeck, C., Vázquez Riveiros, N., Hodell, D.A., 2016. Evolution of South Atlantic density and chemical stratification across the last deglaciation. Proc. Natl. Acad. Sci. Unit. States Am. 113, 514. https://doi.org/10.1073/pnas.1511252113.
Robinson, L.F., Adkins, J.F., Keigwin, L.D., Southon, J., Fernandez, D.P., Wang, S.L., Scheirer, D.S., 2005. Radiocarbon variability in the western North atlantic during the last deglaciation. Science 310, 1469. https://doi.org/10.1126/science.1114832.
Robinson, L.F., van de Flierdt, T., 2009. Southern Ocean evidence for reduced export of north atlantic deep water during Heinrich event 1. Geology 37, 195–198. https://doi.org/10.1130/g25363a.1.
Rogerson, M., Colmenero-Hidalgo, E., Levine, R.C., Rohling, E.J., Voelker, A.H.L., Bigg, G.R., Schönfeld, J., Cacho, I., Sierro, F.J., Löwemark, L., Reguera, M.I., de Abreu, L., Garrick, K., 2010. Enhanced Mediterranean-Atlantic exchange during Atlantic freshening phases. G-cubed 11, Q08013. https://doi.org/10.1029/2009gc002931.
Sarafanov, A., Falina, A., Mercier, H., Sokov, A., Lherminier, P., Gourcuff, C., Gladyshev, S., Gaillard, F., Daniault, N., 2012. Mean full-depth summer circulation and transports at the northern periphery of the Atlantic Ocean in the 2000s. J. Geophys. Res. 117, C01014. https://doi.org/10.1029/2011jc007572.
Sarnthein, M., Winn, K., Duplessy, J.-C., Fontugne, M.R., 1988. Global variations of surface ocean productivity in low and mid latitudes: influence on CO2 reservoirs of the deep ocean and atmosphere during the last 21,000 years. Paleoceanography 3, 361–399. https://doi.org/10.1029/PA003i003p00361.
Sarnthein, M., Winn, K., Jung, S.J.A., Duplessy, J.-C., Labeyrie, L., Erlenkeuser, H., Ganssen, G., 1994. Changes in east Atlantic deepwater circulation over the last 30000 years: eight time slice reconstructions. Palaeoceanography 9, 209–267. https://doi.org/10.1029/93PA03301.
Schlitzer, R., 2012. Ocean Data View. http://odv.awi.de.
Schmidt, M.W., Lynch-Stieglitz, J., 2011. Florida Straits deglacial temperature and salinity change: implications for tropical hydrologic cycle variability during the Younger Dryas. Paleoceanography 26, PA4205. https://doi.org/10.1029/2011pa002157.
Schmittner, A., Bostock, H.C., Cartapanis, O., Curry, W.B., Filipsson, H.L., Galbraith, E.D., Gottschalk, J., Herguera, J.C., Hoogakker, B., Jaccard, S.L., Lisiecki, L.E., Lund, D.C., Martínez-Méndez, G., Lynch-Stieglitz, J., Mackensen, A., Michel, E., Mix, A.C., Oppo, D.W., Peterson, C.D., Repschläger, J., Sikes, E.L., Spero, H.J., Waelbroeck, C., 2017. Calibration of the carbon isotope composition (δ13C) of benthic foraminifera. Paleoceanography 32, 512–530. https://doi.org/10.1002/2016PA003072.
Schmittner, A., Lund, D.C., 2015. Early deglacial Atlantic overturning decline and its role in atmospheric CO2 rise inferred from carbon isotopes ($\delta^{13}C$). Clim. Past 11, 135–152. https://doi.org/10.5194/cp-11-135-2015.
Schmitz, W.J., McCartney, M.S., 1993. On the north atlantic circulation. Rev. Geophys. 31, 29–49. https://doi.org/10.1029/92RG02583.
Schönfeld, J., 1997. The impact of the Mediterranean Outflow Water (MOW) on benthic foraminiferal assemblages and surface sediments at the southern Portuguese continental margin. Mar. Micropaleontol. 29, 211–236. https://doi.org/10.1016/S0377-8398(96)00050-3.
Schönfeld, J., Zahn, R., 2000. Late Glacial to Holocene history of the Mediterranean Outflow. Evidence from benthic foraminiferal assemblages and stable isotopes at the Portuguese margin. Palaeogeogr. Palaeoclimatol. Palaeoecol. 159, 85–111. https://doi.org/10.1016/S0031-0182(00)00035-3.
Schott, F., Zantopp, R., Stramma, L., Dengler, M., Fischer, J., Wibaux, M., 2004. Circulation and deep-water export at the western exit of the subpolar North Atlantic. J. Phys. Oceanogr. 34, 817. https://doi.org/10.1175/1520-0485(2004)034<0817:CADEAT>2.0.CO;2.
Schott, F.A., Brandt, P., 2013. Circulation and Deep Water Export of the Subpolar

North Atlantic during the 1990's.
Schwab, C., Kinkel, H., Weinelt, M., Repschläger, J., 2012. Coccolithophore paleoproductivity and ecology response to deglacial and Holocene changes in the Azores Current System. Paleoceanography 27, PA3210. https://doi.org/10.1029/2012pa002281.
Serrano, O., Serrano, L., Mateo, M.A., 2008. Effects of sample pre-treatment on the δ13C and δ18O values of living benthic foraminifera. Chem. Geol. 257, 218–220. https://doi.org/10.1016/j.chemgeo.2008.09.013.
Shackleton, N.J., 1974. Attainment of isotopic equilibrium ocean water and the benthonic foraminifera genus Uvigerina: isotopic changes in the ocean during the last glacial. Cent. Natl.Rech. Sci. Colloq. Int. 219, 203–209.
Shackleton, N.J., Opdyke, N.D., 1973. Oxygen isotope and palaeomagnetic stratigraphy of Equatorial Pacific core V28-238: oxygen isotope temperatures and ice volumes on a 105 year and 106 year scale. Quat. Res. 3, 39–55.
Shakun, J.D., Clark, P.U., He, F., Marcott, S.A., Mix, A.C., Liu, Z., Otto-Bliesner, B., Schmittner, A., Bard, E., 2012. Global warming preceded by increasing carbon dioxide concentrations during the last deglaciation. Nature 484, 49–54. https://doi.org/10.1038/nature10915.
Shimmield, G., 2004. Stable isotope analysis on planktic foraminifera in sediment core BOFS17K. In: Lowry, Roy K., Machin, P. (Eds.), Compilation of the Results of EU-Project BOFS. PANGAEA. https://doi.org/10.1594/PANGAEA.859221 (PANGAEA).
Sierro, F.J., Hodell, D.A., Curtis, J.H., Flores, J.A., Reguera, I., Colmenero-Hidalgo, E., Bárcena, M.A., Grimalt, J.O., Cacho, I., Frigola, J., Canals, M., 2005. Impact of iceberg melting on Mediterranean thermohaline circulation during Heinrich events. Paleoceanography 20. https://doi.org/10.1029/2004PA001051.
Sigman, D.M., Boer, A.M.D., Haug, G.H., 2007. Antarctic Stratification, Atmospheric Water Vapor, and Heinrich Events: a Hypothesis for Late Pleistocene Deglaciations, Ocean Circulation: Mechanisms and Impacts—Past and Future Changes of Meridional Overturning, pp. 335–349.
Sigman, D.M., Hain, M.P., Haug, G.H., 2010. The polar ocean and glacial cycles in atmospheric CO2 concentration. Nature 466, 47–55. https://doi.org/10.1038/nature09149.
Skinner, L.C., Fallon, S., Waelbroeck, C., Michel, E., Barker, S., 2010. Ventilation of the deep Southern Ocean and deglacial CO2 rise. Science 328, 1147–1151. https://doi.org/10.1126/science.1183627.
Skinner, L.C., Shackleton, N.J., 2006. Deconstructing Terminations I and II: revisiting the glacioeustatic paradigm based on deep-water temperature estimates. Quat. Sci. Rev. 25, 3312–3321. https://doi.org/10.1016/j.quascirev.2006.07.005.
Slowey, N.C., Curry, W.B., 1995. Glacial-interglacial differences in circulation and carbon cycling within the upper western North-Atlantic. Paleoceanography 10, 715–732. https://doi.org/10.1029/95PA01166.
Solignac, S., de Vernal, A., Hillaire-Marcel, C., 2004. Holocene sea-surface conditions in the North Atlantic—contrasted trends and regimes in the western and eastern sectors (Labrador Sea vs. Iceland Basin). Quat. Sci. Rev. 23, 319–334. https://doi.org/10.1016/j.quascirev.2003.06.003.
Stein, K., Timmermann, A., Kwon, E.Y., Friedrich, T., 2020. Timing and magnitude of Southern Ocean sea ice/carbon cycle feedbacks. Proc. Natl. Acad. Sci. Unit. States Am. 117, 4498. https://doi.org/10.1073/pnas.1908670117.
Struve, T., Roberts, N.L., Frank, M., Piotrowski, A.M., Spielhagen, R.F., Gutjahr, M., Teschner, C., Bauch, H.A., 2019. Ice-sheet driven weathering input and water mass mixing in the Nordic Seas during the last 25,000 years. Earth Planet Sci. Lett. 514, 108–118. https://doi.org/10.1016/j.epsl.2019.02.030.
Talley, L.D., 2013. Closure of the global overturning circulation through the Indian, pacific, and southern oceans: schematics and transports. Oceanography 26, 80–97.
Telesiński, M.M., Spielhagen, R.F., Bauch, H.A., 2014. Water mass evolution of the Greenland Sea since late glacial times. Clim. Past 10, 123–136. https://doi.org/10.5194/cp-10-123-2014.
Tessin, A.C., Lund, D.C., 2013. Isotopically depleted carbon in the mid-depth South Atlantic during the last deglaciation. Paleoceanography. https://doi.org/10.1002/palo.20026.
Thompson, A.F., Hines, S.K., Adkins, J.F., 2019. A Southern Ocean mechanism for the interhemispheric coupling and phasing of the bipolar seesaw. J. Clim. 32, 4347–4365. https://doi.org/10.1175/JCLI-D-18-0621.1.
Thornalley, D., Elderfield, H., McCave, I.N., 2011. Reconstructing North Atlantic deglacial surface hydrography and its link to the Atlantic overturning circulation. Global Planet. Change 79, 163–175. https://doi.org/10.1016/j.gloplacha.2010.06.003.
Thornalley, D., McCave, I.N., Elderfield, H., 2010. Freshwater input and abrupt deglacial climate change in the North Atlantic. Paleoceanography 25, PA1201. https://doi.org/10.1029/2009PA001772.
Thornalley, D.J.R., Barker, S., Becker, J., Hall, I.R., Knorr, G., 2013. Abrupt changes in deep Atlantic circulation during the transition to full glacial conditions. Paleoceanography 28, 253–262. https://doi.org/10.1002/palo.20025.
Thornalley, D.J.R., Bauch, H.A., Gebbie, G., Guo, W., Ziegler, M., Bernasconi, S.M., Barker, S., Skinner, L.C., Yu, J., 2015. A warm and poorly ventilated deep Arctic Mediterranean during the last glacial period. Science 349, 706–710. https://doi.org/10.1126/science.aaa9554.
Tiedemann, R., 1991. Acht Millionen Jahre Klimageschichte von Nordwest Afrika und Palāo-Ozeanographie des angrenzenden Atlantiks: Hochauflösende Zeitreihen von ODP-Sites 658-661, Berichte - Reports, Geologisch-Paläontologisches Institut und Museum, Christian-Albrechts-Universität, Kiel. Geologisch-Paläontologisches Institut und Museum, Christian-Albrechts-Universität, Kiel, Kiel, Germany, pp. 1–190.
Tjallingii, R., Claussen, M., Stuut, J.-B.W., Fohlmeister, J., Jahn, A., Bickert, T., Lamy, F., Rohl, U., 2008. Coherent high- and low-latitude control of the northwest African hydrological balance. Nat. Geosci. 1, 670–675. https://doi.org/10.1038/ngeo289.
Våge, K., Pickart, R.S., Sarafanov, A., Knutsen, ò., Mercier, H., Lherminier, P., van Aken, H.M., Meincke, J., Quadfasel, D., Bacon, S., 2011. The Irminger Gyre: circulation, convection, and interannual variability. Deep Sea Res. Oceanogr. Res. Pap. 58, 590–614. https://doi.org/10.1016/j.dsr.2011.03.001.
van Aken, H.M., 2000a. The hydrography of the mid-latitude northeast Atlantic Ocean: I: the deep water masses. Deep Sea Res. Oceanogr. Res. Pap. 47, 757–788. https://doi.org/10.1016/S0967-0637(99)00092-8.
van Aken, H.M., 2000b. The hydrography of the mid-latitude Northeast Atlantic Ocean: II: the intermediate water masses. Deep Sea Res. Oceanogr. Res. Pap. 47, 789–824.
van Aken, H.M., 2001. The hydrography of the mid-latitude Northeast Atlantic Ocean – Part III: the subducted thermocline water mass. Deep Sea Res. Oceanogr. Res. Pap. 48, 237–267. https://doi.org/10.1016/S0967-0637(00)00059-5.
Van Aken, H.M., De Boer, C.J., 1995. On the synoptic hydrography of intermediate and deep water masses in the Iceland Basin. Deep Sea Res. Oceanogr. Res. Pap. 42, 165–189.
van Kreveld, S., Sarnthein, M., Erlenkeuser, H., Grootes, P., Jung, S., Nadeau, M.J., Pflaumann, U., Voelker, A., 2000. Potential links between surging ice sheets, circulation changes, and the dansgaard-oeschger cycles in the Irminger Sea, 60-18 kyr. Paleoceanography 15, 425–442. https://doi.org/10.1029/1999pa000464.
van Sebille, E., Baringer, M.O., Johns, W.E., Meinen, C.S., Beal, L.M., de Jong, M.F., van Aken, H.M., 2011. Propagation pathways of classical Labrador Sea water from its source region to 26°N. J. Geophys. Res. 116, C12027. https://doi.org/10.1029/2011jc007171.
Vetter, L., Spero, H.J., Eggins, S.M., Williams, C., Flower, B.P., 2017. Oxygen isotope geochemistry of Laurentide ice-sheet meltwater across Termination I. Quat. Sci. Rev. 178, 102–117. https://doi.org/10.1016/j.quascirev.2017.10.007.
Vidal, L., Labeyrie, L.D., Cortijo, E., Arnold, M., Duplessy, J.-C., Michel, E., Becqué, S., T C E v W, 1997. Evidence for changes in north atlantic deep water linked to meltwater surges during the Heinrich events. Earth Planet Sci. Lett. 146, 13–27. https://doi.org/10.1016/S0012-821X(96)00192-6.
Voelker, A.H.L., Lebreiro, S.M., Schönfeld, J., Cacho, I., Erlenkeuser, H., Abrantes, F., 2006. Mediterranean outflow strengthening during northern hemisphere coolings: a salt source for the glacial Atlantic? Earth Planet Sci. Lett. 245, 39–55.
Vogelsang, E., Sarnthein, M., Pflaumann, U., 2001. d18O Stratigraphy, Chronology, and Sea Surface Temperatures of Atlantic Sediment Records (GLAMAP-2000 Kiel), Berichte - Reports. Institut für Geowissenschaften. Institut für Geowissenschaften, Christian-Albrechts-Universität, Kiel, Kiel, Germany, pp. 1–11.
Voigt, I., Cruz, A.P.S., Mulitza, S., Chiessi, C.M., Mackensen, A., Lippold, J., Antz, B., Zabel, M., Zhang, Y., Barbosa, C.F., Tisserand, A.A., 2017. Variability in mid-depth ventilation of the western Atlantic Ocean during the last deglaciation. Paleoceanography 32, 948–965. https://doi.org/10.1002/2017PA003095.
Vonhof, H.B., de Graaf, S., Spero, H.J., Schiebel, R., Verdegaal, S.J.A., Metcalfe, B., Haug, G.H., 2020. High-precision stable isotope analysis of <5 μg CaCO3 samples by continuous-flow mass spectrometry. Rapid Commun. Mass Spectrom. 34, e8878. https://doi.org/10.1002/rcm.8878.
Waelbroeck, C., Duplessy, J.-C., Michel, E., Labeyrie, L., Paillard, D., Duprat, J., 2001. The timing of the last deglaciation in North Atlantic climate records. Nature 412, 724–727. https://doi.org/10.1038/35089060.
Waelbroeck, C., Levi, C., Duplessy, J.C., Labeyrie, L., Michel, E., Cortijo, E., Bassinot, F., Guichard, F., 2006. Distant origin of circulation changes in the Indian Ocean during the last deglaciation. Earth Planet Sci. Lett. 243, 244–251. https://doi.org/10.1016/j.epsl.2005.12.031.
Waelbroeck, C., Lougheed, B.C., Vazquez Riveiros, N., Missiaen, L., Pedro, J., Dokken, T., Hajdas, I., Wacker, L., Abbott, P., Dumoulin, J.-P., Thil, F., Eynaud, F., Rossignol, L., Fersi, W., Albuquerque, A.L., Arz, H., Austin, W.E.N., Came, R., Carlson, A.E., Collins, J.A., Dennielou, B., Desprat, S., Dickson, A., Elliot, M., Farmer, C., Giraudeau, J., Gottschalk, J., Henderiks, J., Hughen, K., Jung, S., Knutz, P., Lebreiro, S., Lund, D.C., Lynch-Stieglitz, J., Malaizé, B., Marchitto, T., Martínez-Méndez, G., Mollenhauer, G., Naughton, F., Nave, S., Nürnberg, D., Oppo, D., Peck, V., Peeters, F.J.C., Penaud, A., Portilho-Ramos, R.d.C., Repschläger, J., Roberts, J., Rühlemann, C., Salgueiro, E., Sanchez Goni, M.F., Schönfeld, J., Scussolini, P., Skinner, L.C., Skonieczny, C., Thornalley, D., Toucanne, S., Rooij, D.V., Vidal, L., Voelker, A.H.L., Wary, M., Weldeab, S., Ziegler, M., 2019. Consistently dated Atlantic sediment cores over the last 40 thousand years. Scientific Data 6, 165. https://doi.org/10.1038/s41597-019-0173-8.
Waelbroeck, C., Mulitza, S., Spero, H., Dokken, T., Kiefer, T., Cortijo, E., 2005. A global compilation of late Holocene planktonic foraminiferal 18O: relationship between surface water temperature and 18O. Quat. Sci. Rev. 24, 853–868.
Waelbroeck, C., Skinner, L.C., Labeyrie, L., Duplessy, J.C., Michel, E., Vazquez Riveiros, N., Gherardi, J.M., Dewilde, F., 2011. The timing of deglacial circulation changes in the Atlantic. Paleoceanography 26, PA3213. https://doi.org/10.1029/2010pa002007.
Watson, A.J., Naveira Garabato, A.C., 2006. The role of Southern Ocean mixing and upwelling in glacial-interglacial atmospheric CO2 change. Tellus B 58, 73–87. https://doi.org/10.1111/j.1600-0889.2005.00167.x.
Weinelt, M., 1993. Veränderungen der Oberflächenzirkulation im Europäischen Nordmeer während der letzten 60.000 Jahre - Hinweise aus stabilen Isotopen, Berichte aus dem Sonderforschungsbereich 313, Veränderungen der Umwelt - Der Nördliche Nordatlantik. Christian-Albrechts-Universität zu Kiel, Kiel,

Germany, pp. 1–132.
Weldeab, S., Friedrich, T., Timmermann, A., Schneider, R.R., 2016. Strong middepth warming and weak radiocarbon imprints in the equatorial Atlantic during Heinrich 1 and Younger Dryas. Paleoceanography 31, 1070–1082. https://doi.org/10.1002/2016PA002957.
Willamowski, C., 1999. Verteilungsmuster von Spurenmetallen im glazialen Nordatlantik : Rekonstruktion der Nährstoffbilanz anhand von Cadmiumkonzentrationen in kalkschaligen Foraminiferen. GEOMAR. Christian-Albrechts-Universität, p. 122.
Wilmes, S.B., Green, J.A.M., Schmittner, A., in review. Carbon isotopes consistent with enhanced vertical mixing in the glacial Atlantic. Nat. Commun..
Wilmes, S.B., Schmittner, A., Green, J.A.M., 2019. Glacial ice sheet extent effects on modeled tidal mixing and the global overturning circulation. Paleoceanography and Paleoclimatology 34, 1437–1454. https://doi.org/10.1029/2019PA003644.
Wunsch, C., 2016. Pore fluids and the LGM ocean salinity—Reconsidered. Quat. Sci. Rev. 135, 154–170. https://doi.org/10.1016/j.quascirev.2016.01.015.
Xu, X., Schmitz Jr., W.J., Hurlburt, H.E., Hogan, P.J., Chassignet, E.P., 2010. Transport of Nordic Seas overflow water into and within the Irminger Sea: an eddy-resolving simulation and observations. J. Geophys. Res. 115, C12048. https://doi.org/10.1029/2010jc006351.
Yashayaev, I., 2007. Hydrographic changes in the Labrador Sea, 1960–2005. Prog. Oceanogr. 73, 242–276. https://doi.org/10.1016/j.pocean.2007.04.015.
Yashayaev, I., Loder, J.W., 2009. Enhanced production of Labrador Sea water in 2008. Geophys. Res. Lett. 36, L01606. https://doi.org/10.1029/2008GL036162.
Zabel, M., Schneider, R.R., Wagner, T., Adegbie, A.T., de Vries, U., Kolonic, S., 2001. Late quaternary climate changes in central africa as inferred from terrigenous input to the Niger fan. Quat. Res. 56, 207–217. https://doi.org/10.1006/qres.2001.2261.
Zahn, R., Sarnthein, M., Erlenkeuser, H., 1987. Benthic isotope evidence for changes of the Mediterranean outflow during the Late Quaternary. Paleoceanography 2, 543–559. https://doi.org/10.1029/PA002i006p00543.
Zarriess, M., Johnstone, H., Prange, M., Steph, S., Groeneveld, J., Mulitza, S., Mackensen, A., 2011. Bipolar seesaw in the northeastern tropical Atlantic during Heinrich stadials. Geophys. Res. Lett. 38, L04706. https://doi.org/10.1029/2010gl046070.
Zarriess, M., Mackensen, A., 2011. Testing the impact of seasonal phytodetritus deposition on δ13C of epibenthic foraminifer Cibicidoides wuellerstorfi: a 31,000 year high-resolution record from the northwest African continental slope. Paleoceanography 26. https://doi.org/10.1029/2010PA001944.
Zhang, J., Liu, Z., Brady, E.C., Oppo, D.W., Clark, P.U., Jahn, A., Marcott, S.A., Lindsay, K., 2017. Asynchronous warming and δ18O evolution of deep Atlantic water masses during the last deglaciation. Proc. Natl. Acad. Sci. Unit. States Am. 114, 11075. https://doi.org/10.1073/pnas.1704512114.
Zhang, Y., Chiessi, C.M., Mulitza, S., Zabel, M., Trindade, R.I.F., Hollanda, M.H.B.M., Dantas, E.L., Govin, A., Tiedemann, R., Wefer, G., 2015. Origin of increased terrigenous supply to the NE south American continental margin during Heinrich stadial 1 and the younger dryas. Earth Planet Sci. Lett. 432, 493–500. https://doi.org/10.1016/j.epsl.2015.09.054.
Zhao, N., Marchal, O., Keigwin, L., Amrhein, D., Gebbie, G., 2018. A synthesis of deglacial deep-sea radiocarbon records and their (In)Consistency with modern ocean ventilation. Paleoceanography and Paleoclimatology 33, 128–151. https://doi.org/10.1002/2017PA003174.
Zhao, N., Oppo, D.W., Huang, K.-F., Howe, J.N.W., Blusztajn, J., Keigwin, L.D., 2019. Glacial–interglacial Nd isotope variability of North Atlantic Deep Water modulated by North American ice sheet. Nat. Commun. 10, 5773. https://doi.org/10.1038/s41467-019-13707-z.